SIT-DL-71-1514

IMPACT LOADS ON WARPED PLANING SURFACES LANDING ON SMOOTH AND ROUGH WATER

Final Report

March 1971

by

John A. Mercier

Prepared under Contract N00600-69-C-1072, Task Order 1
for
Naval Air Systems Command
Department of the Navy

DAVIDSON LABORATORY
Stevens Institute of Technology
Castle Point Station
Hoboken, New Jersey 07030

UNCLASSIFIED

Security Classification

DOCUMENT CONTROL DATA · R & D

(Security classification of title, body of abstract and indexing annotation must be entered when the overall report is classified)

ORIGINATING ACTIVITY (Corporate author)

DAVIDSON LABORATORY
STEVENS INSTITUTE OF TECHNOLOGY
CASTLE POINT STATION, HOBOKEN, NEW JERSEY 07030

2a. REPORT SECURITY CLASSIFICATION

UNCLASSIFIED

2b. GROUP

REPORT TITLE

IMPACT LOADS ON WARPED PLANING SURFACES LANDING ON SMOOTH AND ROUGH WATER.

DESCRIPTIVE NOTES (Type of report and inclusive dates)

FINAL

AUTHOR(S) (First name, middle initial, last name)

John A. Mercier

REPORT DATE	7a. TOTAL NO. OF PAGES	7b. NO. OF REFS
March 1971.	viii+28+16 figures	8

8a. CONTRACT OR GRANT NO.	9a. ORIGINATOR'S REPORT NUMBER(S)
N00600-69-C-1072, Task Order 1.	
b. PROJECT NO. DL 3631/318.	Report SIT-DL-71-1514
c.	9b. OTHER REPORT NO(S) (Any other numbers that may be assigned this report)
d.	

10. DISTRIBUTION STATEMENT

This document has been approved for public release and sale; its distribution is unlimited. Application for copies may be made to the Defense Documentation Center, Cameron Station, 5010 Duke Street, Alexandria, Virginia 22314

11. SUPPLEMENTARY NOTES	12. SPONSORING MILITARY ACTIVITY
	Department of the Navy Naval Air Systems Command Washington, D.C. 20360

13. ABSTRACT

The impact of planing surfaces on waves is analyzed according to an extension of the theory for smooth-water impacts in a way that takes account of the influence of wave kinematics. Impacts of the type incurred by seaplanes, in which the weight of the craft is sustained by wing lift, are studied. Data for planing, which is a special case of impact, are used to obtain the needed relationship between virtual mass and hull geometry.

Impact tests with two models having different amounts of warp, or longitudinal variation of deadrise, are compared with theoretical calculations. It is felt that the chines-dry planing characteristics used in the calculations, which were obtained by extrapolation of chines-wet data, are overestimated; more so for the high-warp model than for the low-warp model. Certain observations are made concerning the influence of trim, deadrise, beam loading, glide path, warp rate and waves on the initial stages of the impact, when the vertical velocity is practically uniform, on the basis of the derived differential equation of motion. Complete calculations for impact in waves have not yet been carried out.

Additional experiments to determine the effect of warp rate on chines-dry planing characteristics would be very useful.

DD FORM 1 NOV 68 1473 (PAGE 1)

S/N 0101-807-6811

UNCLASSIFIED

Security Classification

A-31408

14 KEY WORDS	LINK A		LINK B		LINK C	
	ROLE	WT	ROLE	WT	ROLE	WT
Impact						
Planing						
Seaplane Impact						
Impact in Waves						

DAVIDSON LABORATORY

Report SIT-DL-71-1514

March 1971

IMPACT LOADS ON WARPED PLANING SURFACES LANDING ON SMOOTH AND ROUGH WATER

by John A. Mercier

Prepared for the
U.S. Naval Air Systems Command
Department of the Navy
Contract N00600-69-C-1072, Task Order 1
(DL Project 3631/318)

Approved

Daniel Savitsky
Assistant Director

viii + 28 pp.
16 figures

ABSTRACT

The impact of planing surfaces on waves is analyzed according to an extension of the theory for smooth-water impacts in a way that takes account of the influence of wave kinematics. Impacts of the type incurred by seaplanes, in which the weight of the craft is sustained by wing lift, are studied. Data for planing, which is a special case of impact, are used to obtain the needed relationship between virtual mass and hull geometry.

Impact tests with two models having different amounts of warp, or longitudinal variation of deadrise are compared with theoretical calculations. It is felt that the chines-dry planing characteristics used in the calculations, which were obtained by extrapolation of chines-wet data, were overestimated; more so for the high-warp model than for the low-warp model. Certain observations are made concerning the influence of trim, deadrise, beam loading, glide path, warp rate and waves on the initial stages of the impact, when the vertical velocity is practically uniform, on the basis of the derived differential equation of motion. Complete calculations for impact in waves have not yet been carried out.

Additional experiments to determine the effect of warp rate on chines-dry planing characteristics would be very useful.

KEYWORDS

Impact
Planing
Seaplane Impact
Impact in Waves

TABLE OF CONTENTS

NOMENCLATURE

A	amplitude of wave elevation, ft
a	a factor defined by Eq. (4)
b	maximum beam at chine, ft
C_{Δ_o}	static beam loading coefficient, $\Delta_o/\rho g b^3$
C_{Lb}	planing lift coefficient, $L/\frac{1}{2}\rho V^2 b^2$
c	wave celerity, ft/sec
e	base of natural logarithms
F	force (with subscript denoting component), lb
g	acceleration due to gravity, 32.2 ft/sec^2
L	planing lift, normal to undisturbed watersurface, lb
L_s	keel wetted length, ft
m	mass of seaplanes, slugs (also, a variable)
m_w	virtual mass, slugs
p	impact parameter, $\dot{y}/\dot{s}\ \sin\tau$
$\dot{s}$	instantaneous horizontal velocity of seaplane, ft/sec
T	instantaneous draft of seaplane, measured in vertical direction from water surface to point of step, for impact in waves, ft
t	elapsed time, sec
V	instantaneous resultant velocity of seaplane, ft/sec
W	total weight of test model and apparatus moving vertically, lb
w	a factor defined by Eq. (47)
$\dot{x}$	instantaneous velocity of seaplane, parallel to keel, ft/sec
$\dot{y}$	instantaneous velocity of seaplane, normal to keel, ft/sec
z	instantaneous depth of seaplane measured from point of initial contact with water surface to point of step in vertical direction (draft for smooth-water impact), ft

$\dot{z}$	instantaneous vertical velocity, ft/sec
α	a factor defined by Eq. (39)
β	deadrise angle, deg
γ	effective trim angle
Δ_o	seaplane weight, lb
δ	draft-beam ratio, z/b (or T/b)
ϵ	a factor defined by Eq. (33)
ζ	a factor defined by Eq. (36)
η	wave elevation, ft
Λ	wave length, ft
λ	keel wetted length-beam ratio, L_s/b
λ'	mean wetted length-beam ratio, described by Eq. (47)
μ	virtual mass-seaplane mass ratio, m_w/m
ξ	horizontal distance from wave crest to transom
ρ	mass density of water, slugs/cu ft
τ	trim angle of keel relative to horizontal, deg
φ	phi function, $\varphi(m) = m\, e^{1/m}$

SUBSCRIPTS

crit	corresponding to transition from chines-dry to chines-wet condition
i	values for beginning of interval of integration
max	at maximum draft, $\dot{z}=0$
0	initial conditions at water contact, t=0

INTRODUCTION

This report covers a study of water impact of planing surfaces for smooth- and rough-water. Impacts of the type incurred by seaplanes, in which the weight of the craft is sustained entirely (or almost entirely) by wing lift, are studied in particular. The influence of planing surface warp, or varying deadrise, is especially considered.

The present research covers both analytical and experimental work. The brief experimental program was conducted in both smooth water and in waves of two different lengths, using two available warped planing surfaces, having longitudinal warp rates of 3-deg per beam of length and 9-deg per beam of length. The tests were not comprehensive in that a relatively small number of initial conditions (trim, glide angle, velocity, etc.) were covered, but they provide information which can be compared with results of analysis and from which some indications of the influence of warp rate can be obtained

The analysis of seaplane impact may be carried out along somewhat heuristic lines, according to which it is supposed that the seaplane's momentum is imparted to a certain mass of water known as the virtual (or added) mass, which is associated with the seaplane during its contact with the water and that, due to the forward velocity of the seaplane, some of the momentum imparted to the virtual mass is shed behind the seaplane in the form of a wake. Brown,[1] Smiley,[2] Monaghan and Crewe,[3] and others, have developed this analysis for smooth water. In the present report the case of landing at an arbitrary position on a wavy sea surface is analyzed according to a similar procedure, taking account of the influence of the waves on the kinematics of the impact phenomena. Smiley[2] and Brown[1] to a greater extent make use of the fact that steady-state planing

---

[1] Superior numbers in text matter refer to similarly numbered references located in a list at the end of this report.

is a special case of impact and use planing data to obtain the relationship between virtual mass and hull geometry. This procedure is followed in this report, using as-yet-unpublished data obtained by Brown for the warped planes tested.

A brief comparison of impact test results with the analytical procedures is made and the agreement for the smooth-water impacts is reasonable for a model with low warp rate but not as good for a more highly warped model. The planing data for the chines-dry condition, which was extrapolated from chines-wet tests, is suspected of being improperly estimated. This theory has been evaluated for the initial stages of the impact in waves and reasonable correlation is obtained with the results of experiments. The evaluation of this rather complicated theory which takes account of the wave kinematics ought to be carried out to obtain complete time histories of impact accelerations and to obtain a more complete assessment of the method's adequacy.

This work was sponsored by the U.S. Naval Air Systems Command, under Contract N00600-69-C-1072, Task Order 1 (DL Project 3631/318).

THEORY

The impact of a high-speed craft, such as a seaplane, onto the surface of water entails the imparting of momentum from the craft to a certain (figurative) mass of water known as the virtual (or added) mass. Due to the forward velocity of the seaplane, some of the momentum imparted to the virtual mass is shed behind the craft in the form of a wake and is therefore irrecoverable in, for example, the seaplane's rebound from the water. With this hypothesis, it is possible to set up the differential equation of motion governing the impact and, if the virtual mass can be determined for desired cases, to integrate them.

A procedure for evaluating the necessary virtual mass which exploits the fact that planing is a particular case of impact has been developed by Brown[1] and Smiley.[2] Empirical data on planing characteristics of hull geometries of interest are required to fully exploit this concept. These data are fully sufficient for impacts on smooth water but for the rough-water case, further analysis is required. The results of analysis will be outlined first for the smooth-water case with details omitted since they are covered elsewhere,[1,2,3] while alternative rough-water modification of the theory will be treated separately.

Smooth-Water Analysis

The analysis of landing impacts for two cases, (a) constant horizontal velocity component and (b) constant velocity component parallel to keel during impact, has been presented by Monaghan and Crewe.[3] The following additional assumptions are made:

(I) The trim remains constant throughout the impact.

(II) Inertia forces predominate. Thus, gravity and viscous forces are neglected and the loads act normal to the keel.

(III) The float has a weightless mass; that is, the weight of the float is supported by wing lift throughout the impact.

(iv) The virtual mass is a function of the geometry of the float in contact with the water only; e.g., $m_w = f(z)$.

(v) The water surface is initially smooth.

The impacting float is shown in Fig. 1, together with the symbols used in the analysis. Brown's[1] analysis, with the symbols and configuration delineated in Fig. 1, is as follows:

$$\text{The resultant force normal to the keel } F_y = \left\{\begin{array}{l}\text{Total rate of change of momentum}\\ \text{of virtual mass of fluid}\end{array}\right.$$

and

$$\left.\begin{array}{l}\text{Total rate of change}\\ \text{of momentum of virtual}\\ \text{mass of fluid}\end{array}\right\} = \left\{\begin{array}{l}\text{Rate of change of}\\ \text{momentum of}\\ \text{virtual mass, } m_w,\\ \text{under float}\end{array}\right\} + \left\{\begin{array}{l}\text{Rate of shedding}\\ \text{of momentum of}\\ \text{virtual mass}\\ \text{to wake}\end{array}\right.$$

$$F_y = \frac{d}{dt}(m_w \dot{y}) + \left(\frac{dm_w}{dL}\right)_{L=L_s} \dot{x}\dot{y} \qquad (1)$$

The vertical component of the force due to water impact is

$$F_z = F_y \cos\tau \qquad (2)$$

The details of the further development of the analysis differ somewhat for two alternate cases:

(a) constant horizontal velocity, $\dot{s}$ = constant

or (b) constant velocity component parallel to keel, $\dot{x}$ = constant

The following differential equation describes the motion:

$$-\frac{\ddot{y}}{\dot{y}^2} = \frac{\cos\tau}{a + \mu}\frac{d\mu}{dz} \qquad (3)$$

where μ is the virtual mass, expressed as a fraction of the mass of the craft, $\mu = m_w/m$, and the factor a has a different value for the two cases

(a) $\dot{s}$ = constant, $a = \sec^2\tau$

(b) $\dot{x}$ = constant, $a = 1.0$ (4)

A solution method adopted by Brown[1] for this equation is to make a substitution of variables which, for case (a), $\dot{s}$ = constant, becomes:

Let

$$p = \dot{y}/\dot{s} \sin\tau \tag{5}$$

$$\dot{p} = \ddot{y}/\dot{s} \sin\tau \tag{6}$$

Also, since

$$\dot{z} = \dot{y} \sec\tau - \dot{s} \tan\tau \tag{7}$$

$$\dot{z} = (p-1)\, \dot{s} \tan\tau \tag{8}$$

Then, Eq. (3) becomes

$$\frac{-\dot{p}\,(p-1)}{p^2} \sec\tau = \frac{\cos\tau}{(\sec^2\tau + \mu)} \frac{d\mu}{dz} \frac{dz}{dt} \tag{9}$$

or

$$-\frac{dp}{p^2}(p-1) = \frac{\cos^2\tau}{(\sec^2\tau + \mu)}\, d\mu \quad . \tag{10}$$

Integration of Eq. (10) gives

$$-\log p - \frac{1}{p}\Big|_{p_o}^{p} = \cos^2\tau \log(\sec^2\tau + \mu)\Big|_{\mu=0}^{\mu} \tag{11}$$

or

$$\frac{p_o e^{1/p_o}}{p\, e^{1/p}} = (1 + \mu \cos^2\tau)^{\sec^2\tau} \quad ; \tag{12}$$

defining

$$\varphi(m) \equiv m\, e^{1/m} \quad , \tag{13}$$

$$\varphi(p) = \varphi(p_o)/(1+\mu\cos^2\tau)^{\sec^2\tau} \tag{14}$$

or

$$p = \varphi^{-1}\left[\frac{\varphi(p_o)}{(1+\mu\cos^2\tau)^{\sec^2\tau}}\right] \quad . \tag{15}$$

The vertical acceleration is found as

$$\ddot{z} = -\left(\frac{\dot{y}_o^2}{p_o^3}\right)\left\{\varphi^{-1}\left[\frac{\varphi(p_o)}{(1+\mu\cos^2\tau)^{\sec^2\tau}}\right]\right\}^2 \frac{1}{\sec^2\tau + \mu} \frac{d\mu}{dz} \tag{16}$$

The vertical velocity can be evaluated as

$$\frac{\dot{z}}{\dot{z}_o} = \frac{p - 1}{p_o - 1} = \frac{\varphi^{-1}\left[\dfrac{\varphi(p_o)}{(1+\mu\cos^2\tau)^{\sec^2\tau}} - 1\right]}{p_o - 1} \tag{17}$$

At maximum draft $\dot{z} = 0$, and the corresponding added mass function is obtained as

$$\mu_{max} = \sec^2\tau\left[\left(\frac{\varphi(p_o)}{e}\right)^{\cos^2\tau} - 1\right] \tag{18}$$

The preceding analysis yields expressions for the vertical acceleration, Eq. (16), and the vertical velocity ratio, Eq. (17), during the smooth-water impact in terms of the initial conditions and the virtual mass only. Thus to determine the loads and motions during any particular impact as specified by the initial conditions, it is only necessary to find

$$\mu = f(z)$$

in order that the acceleration and vertical velocity may be plotted against draft. Where a time base is needed, the relation between time and draft is given by:

$$t = \int \frac{dt}{dz}\, dz = \int_o^z \frac{dz}{\dot{z}} \tag{19}$$

an integration which is performed graphically from a plot of $1/\dot{z}$ against z.

The phi-function introduced in Eq. (13) above is tabulated in Table 1, taken from Brown's report,[1] and graphed in Fig. 2, and it may be noted that the inverse phi-function is two valued, values greater than 1 applying to the descent into water and those less than 1 the ascent, each value of p and therefore of virtual mass ... and therefore of draft being encountered twice in an impact.

Determination Of The Virtual Mass

The normal force on the float can be derived from Eq. (1) as

$$F_y = m_w \ddot{y} + \dot{y}^2 \frac{dm_w}{dz} \cos\tau \tag{20}$$

During planing $\ddot{y}=\dot{z}=0$, (Fig. 1), so that

$$\dot{y} = V\sin\tau$$

The lift, $L = F_y\cos\tau$

and $m_w = \mu m = \mu \frac{\Delta_o}{g}$

substituting for $\ddot{y}$, $\dot{y}$, F_y and m_w in Eq. (3)

$$L\sec\tau = V^2\sin^2\tau \frac{d\mu}{dz}\frac{\Delta_o}{g}\cos\tau$$

$$\therefore \quad \frac{d\mu}{dz} = \frac{Lg}{\Delta_o V^2 \sin^2 \cos^2\tau} \tag{21}$$

$$\therefore \quad \frac{d\mu}{dz} = \frac{1}{2C_{\Delta_o} b \sin^2\tau \cos^2\tau} C_{Lb}$$

where $$C_{Lb} = \frac{L}{\frac{1}{2}\rho V^2 b^2}$$

substituting the draft beam ratio $\delta = z/b$ in Eq. (21)

$$\frac{d\mu}{d\delta} = \frac{1}{2C_{\Delta_o} \sin^2\tau \cos^2\tau} C_{L_b}$$

$$\mu = \frac{1}{2C_{\Delta_o} \sin^2\tau \cos^2\tau} \int_o^\delta C_{Lb} d\delta \tag{22}$$

Thus $d\mu/dz$ may be found from Eq. (21) and a plot of C_{L_b} against δ , obtained from planing data, and μ from an integration of this plot, graphical or otherwise, and Eq. (22).

Analysis For Waves

A straightforward extension of Brown's method of analysis to the case of landing in waves may be constructed by referring the craft motion to the wave kinematics. Figure 3 illustrates the velocities and angles at contact on the wave, assuming the influence of the wave is like that of an inclined body of water in horizontal translation. The slope of this body of water may be taken equal to that of the wave at the location of the transom or step of the craft. As an approximation, the virtual mass will be assumed to correspond to that obtained in smooth water for a similar transom immersion and keel wetted length, that is, with trim angle corresponding to the sum of the geometric trim angle of the craft and the wave slope evaluated at, say, the transom.

The kinematic conditions for the impact in waves are sketched in Fig. 3, where the wave motion is described relative to coordinate translating horizontally, but not vertically, with the craft. For the present test program, the landings are carried out in head seas so the wave celerity, c, is additive to the craft velocity, ξ, or the relative wave speed is $\xi + c$; for landings in following seas, the relative speed must be $\xi - c$. The equation of the wave elevation will be taken to be simple harmonic,

$$\eta = A \cos 2\pi\left[\frac{s}{\lambda} + \frac{(\xi \pm c)}{\lambda} t\right] \tag{23}$$

as a reasonable approximation of the wave profiles encountered in the test program, and one which affords analytic simplicity.

The basic equation of motion for uniform horizontal velocity is similar to Eqs. (2),

$$-m\ddot{z} = \cos\tau \left\{\frac{d}{dt}(m_w \dot{y}) + \left(\frac{dm_w}{dL}\right)_{L=L_s} \dot{x}\dot{y}\right\} \tag{24}$$

The virtual mass is to be obtained, as mentioned above, from the planing data as a function of the transom immersion

$$\Upsilon = \delta z + \delta\eta \tag{25}$$

where the δ symbol denotes variation within the interval of time starting from the instant of first contact of the craft and water, and of the "effective" trim angle,

$$\gamma = \tau - d\eta/d\xi \tag{26}$$

The keel wetted length may be expressed as

$$L_s = T/(\sin\tau - \cos\tau \tan d\eta/d\xi) \tag{27}$$

Writing the left side of Eq. (24) in terms of y, we obtain

$$-m\ddot{y} = \cos^2\tau\left[m_w\ddot{y} + \dot{y}\dot{t}\frac{dm_w}{d\tau} + \frac{dm_w}{d\tau}\dot{x}\dot{y}\left(\sin\tau - \cos\tau \tan\frac{dy}{d\xi}\right)\right] \tag{28}$$

and since

$$\dot{t} = \dot{y}\cos\tau - \dot{x}\sin\tau + \dot{\eta} \tag{29}$$

and $$\dot{x}\cos\tau = \dot{s} - \dot{y}\sin\tau$$

then

$$-m\ddot{y} = \cos^2\tau\left\{m_w\ddot{y} + \frac{dm_w}{d\tau}\left[\dot{y}^2\cos\tau + \dot{y}\dot{\eta} - (\dot{y}\dot{s} - \dot{y}^2\sin\tau)\tan\frac{d\eta}{d\xi}\right]\right\} \tag{30}$$

For relatively small amplitude waves ($A/\Lambda < 1/20$) $\tan d\eta/d\xi \approx d\eta/d\xi$ and, substituting appropriate derivatives of Eq. (23) into Eq. (30),

$$-m\ddot{y} = \cos^2\tau\left\{m_w\ddot{y} + \frac{dm_w}{d\tau}\left[\dot{y}^2\cos\tau - \dot{y}(\pm c)\frac{2\pi A}{\Lambda}\sin 2\pi\left(\frac{\xi}{\Lambda} + \frac{(\dot{s}\pm c)}{\Lambda}t\right)\right]\right\} \tag{31}$$

where it has been assumed that $|\dot{y}\sin\tau|$ is negligible compared to wave celerity c, which is certainly valid for typical trim angles and long (high speed waves). Equation (31) may be rewritten as

$$-\ddot{y} = \frac{\cos\tau}{\sec^2\tau + \mu}(\dot{y}^2 - \epsilon\dot{y})\frac{d\mu}{d\tau} \tag{32}$$

where

$$\epsilon = (\pm c)\frac{2\pi A}{\Lambda}\sec\tau \sin 2\pi\left[\frac{\xi_o}{\Lambda} + \frac{(\dot{s}\pm c)}{\Lambda}t\right] \tag{33}$$

A solution method analogous to that adopted by Brown for the smooth-water case, described previously, will be employed again, with the

substitution

$$p = \dot{y}/\$ \sin\tau \tag{5}$$

employed again, leading to

$$-\frac{[(p-1)\$ \tan\tau + \dot{\eta}]\dot{\$}}{p^2\$ \sin\tau - \epsilon p} = \frac{\cos\tau}{\sec^2\tau + \mu}\frac{d\mu}{dt} \tag{34}$$

In case $\dot{\eta}$ and ϵ are zero, as in way of a wave crest or trough, Eq. (34) is the same as Eq. (10) for smooth water. Re-arranging terms,

$$-\frac{dp}{p-\zeta} - \frac{(\dot{\eta}/\$ \tan\tau - 1)dp}{p^2 - \zeta p} = \frac{\cos^2\tau}{\sec^2\tau+\mu} d\mu \tag{35}$$

where

$$\zeta = \frac{\epsilon}{\$ \sin\tau} = \frac{\pm c}{\$}\frac{4\pi A}{\lambda \sin 2\tau} \sin 2\pi\left[\frac{\xi}{\lambda} + \frac{(\$ \pm c)}{\lambda} t\right] \tag{36}$$

The integration of Eq. (35) can be carried out piecewise, assuming ζ and $\dot{\eta}$ do not vary within the interval of integration:

$$-\ln(p-\zeta)\Big|_{p_l}^{p_{l+1}} - (\dot{\eta}/\$ \tan\tau - 1)\frac{1}{\zeta}\ln\frac{p-\zeta}{p}\Big|_{p_l}^{p_{l+1}} = \cos^2\tau \ln(\sec^2\tau+\mu\Big|_{\mu_l}^{\mu_{l+1}} \tag{37}$$

where p_{l+1} is sufficiently close to p_l that $\dot{\eta}$, $\frac{d\eta}{d\xi}$ and therefore, ζ can be approximated as constants within the interval.

This can be rearranged to give

$$\left(\frac{p_{l+1} - \zeta_l}{p_l - \zeta_l}\right)^{1+\alpha_l}\left(\frac{p_l}{p_{l+1}}\right)^{\alpha_l} = \left(\frac{\sec^2\tau + \mu_{l+1}}{\sec^2\tau + \mu_l}\right)^{-\cos^2\tau} \tag{38}$$

where

$$\alpha = (\dot{\eta}/\$ \tan\tau - 1)/\zeta \tag{39}$$

and the subscript l of the quantities α and ζ implies that their values at the beginning of the interval of integration may be used although, according to the mean value theorem an average over the interval may be more appropriate. This solution is not valid when $\zeta = 0$, in which case the smooth-water solution, Eq. (15), applies.

The vertical acceleration is given by

$$-\ddot{z} = \frac{\sin^2\tau\ \dot{s}^2}{\sec^2\tau + \mu}\left[p^2 - \zeta p\right]\frac{d\mu}{dT} \tag{40}$$

and the vertical velocity ratio is the same as for smooth water, viz.,

$$\frac{\dot{z}}{\dot{z}_o} = \frac{p-1}{p_o-1} \tag{17}$$

In this case a numerical solution may be constructed for a particular impact as specified by the initial conditions of the craft and the wave by solving Eq. (38) for the virtual mass μ, for successive increments of the variable p. Knowing the virtual mass, its derivative $d\mu/dT$ may be obtained and, hence, the vertical acceleration from Eq. (40). The corresponding time may be obtained as

$$t = \int \frac{dp}{\dot{p}} = \dot{s}\tan\tau \int \frac{dp}{\ddot{z}} \tag{41}$$

except near the initial contact, when $\ddot{z}=0$. For this very brief duration of the initial interval

$$t_1 = \frac{T_1}{\dot{z}_o + \dot{\eta}_o} \tag{42}$$

where T_1 is the transom immersion corresponding to the added mass evaluated at the end of the first increment of p;

The vertical heave displacement of the craft at the end of each increment may be obtained in two ways,

1. $$z = \int \dot{z}dt \tag{43}$$

and

2. $$z = T(\mu_{i+1}\ ,\ \gamma_{i+1}) - \eta_{i+1} \tag{44}$$

where the values computed from Eqs. (43) and (44) ought to agree or the computations performed with smaller increments of p until they do.

MODELS

Two models, having different amounts of deadrise warp, were tested. Sketches of these models, both of which have the same deadrise at the transom, 10 degrees, are shown in Fig. 4. Both models are made of wood and have a sharp-edged metal insert at the chine to assure flow separation at this location during planing and impacting. These models have previously been tested to obtain steady-state planing force characteristics in smooth water.

TEST PROCEDURE

Apparatus

The planing hull models were tested in Tank No. 3 of the Davidson Laboratory, using the impact apparatus sketched in Fig. 5. This apparatus consists of a pole, free to move vertically, to which the model is attached, and which serves to restrain the model in trim, roll and yaw. The apparatus includes a negator spring: this is a constant torque device to which pulleys of various diameter can be attached so that any required amount of tension can be put into an unloading wire attached to the pole. A solenoid operated pin engages in a series of holes drilled at one inch pitch in the pole. Thus the model can be locked at various heights and released when required by energizing the solenoid. The model is connected to the pole through a trim-adjusting device.

In these tests the weight of the model hull, pole and auxiliary gear was supported by the negator spring, so that once given a downward velocity, the planing hull would continue to fall at constant speed to the limit of travel of the pole or until the model hit the water. Initial vertical velocities were obtained by raising the pole to a point where the unloading wire was pulling down, as shown in Fig. 5. Since the tension in the unloading wire was W (the total weight moving vertically), the total accelerating force in this condition was $2W$. Consequently, when the model was released, a constant 2g acceleration was applied until the point of attachment of the unloading wire to the pole reached the guide pulleys. From this point, a constant velocity was maintained until the model hit the water. By raising the pole to different heights, and thus allowing the constant 2g acceleration to act for varying lengths of time, a range of dropping speeds was obtained.

A wave elevation sensor is attached to a towing carriage at a distance of 78 inches ahead of the vertical pole. Another wave sensor is fixed in the tank, between the tank sidewall and the model track and near the region

of the tank where the model usually impacted during tests.

Measuring Techniques

A continuous record of the height of the model during each run was obtained from a heave indicator. The heave transducer signal was carried by overhead cable to an oscillograph which recorded the heave-time history.

A water contact device was arranged so that when the model's keel contacted the water, an electric circuit was completed and the resulting signal was recorded on the oscillograph tape.

The vertical velocity at first contact and at rebound from the water was obtained by measuring the slope of the heave-time history at these two instants.

A linear accelerometer, having a range of ±100g, was used to obtain time histories of the vertical acceleration during each run. The natural frequency of this accelerometer when filled with damping fluid was about 200 cycles per second, and damping was 70% of critical. In this condition no phase distortion is introduced and the time lag of the accelerometer is of the order of 0.002 seconds. The accelerometer signals were fed by overhead cable to the oscillograph and recorded in the form of an acceleration-time history.

Flow Observation

Still photographs of the spray pattern generated by the impact were obtained with an objective of coordinating the spray observations with the impact oscillograms. The shutter opening was triggered by a switch which was actuated when the towing carriage reached a certain position along the tank length, several feet after the solenoid operated pin released the heave pole. Photographs were obtained at somewhat similar instants after first contact with the water, varying with initial heave pole height (acceleration distance), trim angle, and position of model relative to wave profile.

Setup

A photograph of the complete setup is shown in Fig. 6.

Test Program

In the test runs the model was first raised to the required dropping height and locked with the solenoid pin. After the carriage reached a steady test speed, usually around 20 ft/sec,a switch actuated the solenoid release at a specific position along the length of the tank. The acceleration, heave and stationary and moving wave wire signals were recorded prior to and during the resulting motion. A photograph of the spray pattern of the impact was obtained for most of the test runs. Trim angles varied from 2 to about 6 degrees while glide-path angles varied from about 9 to 15 degrees. The dropping weight from Model 1 was 19.6 lbs while that for Model 2 was 34.2 lbs, the difference being due to the greater massiveness required for rigidity of the high-warp model.

Impacts on various positions in the oncoming wave profile were affected by repeat runs started at slightly different phases of the stationary wave wire signal. Regular waves were used throughout these tests.

Precision

The test parameters were set with the following precision:

Weight = ± 0.10 lb

Trim = ± 0.2 deg

The measured quantities were determined with the following precision:

Horizontal Speed	± 0.03 ft/sec
Initital Vertical Velocity	± 0.1 ft/sec
Maximum Vertical Acceleration	± 0.6 ft/sec^2
Time to Maximum Acceleration	± 0.01 sec
Maximum Draft	± 0.02 ft
Wave Elevation	± 0.01 ft
Wave Period	± 0.01 sec

While static calibration of the accelerometer indicated a precision of the order of ±3 ft/sec^2, it was found that when the accelerometer was mounted on the carriage and run at test speeds, a "noise" signal having an amplitude of around 10 ft/sec^2 was picked up which lowered the precision with which the peak and other acceleration characteristics could be determined. No quantitative estimate of the probable experimental error of the results has been made.

PLANING DATA FOR VIRTUAL MASS

The theoretical justification for using steady planing data for the evaluation of the virtual mass which is necessary in the impact analysis has been given above. Appropriate data for particular hull geometries must be adapted for numerical evaluations of the analytical results.

There are, to be sure, a large number of formulations describing planing lift which could be employed, most of which are rather limited in range of applicability (type of geometry, trim angle, speed, etc.). For landing impacts of seaplanes, data and formulations for high-speed planing, where buoyant lift is negligibly small, are appropriate. Two distinctive phases of planing of deadrise surfaces may be distinguished: "dry-chine" and "wet-chine" characterized by the illustrations of Figs. 7a and 7b. Flat plate, or zero-deadrise surfaces exhibit some other interesting planing features but hulls of this geometry are not common and we may consider only the two abovementioned phases.

Brown[4] has investigated the low wetted length, or chines-dry, planing condition, using data available in 1954. This phase is, of course, of crucial importance to the seaplane landing analysis where the craft enters the water from the air, an all dry condition. Brown's analysis[4] leads to a relatively simple expression for the planing lift of a wedge with constant deadrise angle, β .

$$C_{L_b} = 3.6\delta^2 \sin\tau \cos\tau(1-\sin\tau) \cot^2\beta \qquad (45)$$

The principal theoretical assumptions leading to the form of this expression are that the lift is directly proportional to the area below the still waterline and that the lift coefficient based on area is proportional to the square of the sine of the trim angle (as for extremely low aspect ratio wings, see Milne-Thomson[5]). The factors 3.6 and $(1-\sin\tau)$ are empirical, and it may be noted that very little new low-wetted-length planing data have been published in the time since Brown's 1954 report.

For chines-wet planing, Brown[6] has recently developed improved formulae for planing lift, based on Shuford's[7] theoretical analysis and new data developed at Davidson Laboratory for constant deadrise planing surfaces, which for very high speeds reduce to

$$C_{L_b} = .785 \sin 2\tau \cos\tau[(1-\sin\beta)\lambda'/(1+\lambda') + .424\lambda' \sin 2\tau \cos\beta] \quad (46)$$

where

$$\lambda' = \lambda + 0.03 - 0.5w - 0.1 \exp[-(\lambda-w)/.03]$$

with

$$w = (0.57 + 0.001\beta)(\tan\beta/2\tan\tau - 0.006\beta) \quad (47)$$

and

$$\delta = \lambda \sin\tau$$

the exponential term is only significant for chine wetted lengths less than one beam.

For the impact study the transition from chines dry to chines wet, planing is important inasmuch as most impacts entail some chine wetting. It has been found[5] that the "critical" wetted length corresponds to the condition when the still waterline passes through the chine point (see Fig. 7a), so that

$$\lambda_{crit} = \frac{b}{2} \cot\tau \tan\beta \quad (48)$$

In the present work the influence of varying deadrise, or warp, is to be studied, and impact tests have been carried out with two models, both of which incorporate warp. Experimental planing data have been obtained for these hulls as part of a different investigation and are plotted in the form of C_{L_b} versus transom draft for the high warp and low warp hulls in Figs. 8 and 9. The data presented are for the highest test speed, $V \cong \sqrt{7gb}$, where static lift due to buoyancy is unimportant. A brief comparison of the influence of warp on the planing data, both for chines-wet and for chines-dry conditions will be presented.

First, it may be noted that there are practically no data for these warped hulls in the chines-dry regime. It has been assumed that the lift in this range is proportional to the square of the draft, as in Eq. (45), passing through the curves of chines-wet planing data at a draft corresponding to λ_{crit} given by Eq. (48), where the transom deadrise angle, β, is

10 degrees. The trim angle dependence is not quite like that given for unwarped hulls in Eq. (45), but is obtained from the empirical curves. Equations describing this lift data have not yet been developed but are not necessary for the extent of computational work to be undertaken for this report.

A comparison of the lift data for hulls having transom deadrise of 10 degrees, 6-deg trim and various warp rates is shown in Fig. 10. The equations for the unwarped planing lift for chines-dry and chines-wet conditions, Eqs. (45) and (46), respectively, do not agree for the critical wetted length given by Eq. (48). Inasmuch as these formulations were developed at different times, and based on different data, it is not remarkable that the relatively minor discrepancies occur. It may be preferred to modify the empirical factor of Eq. (45) so that the chines-dry lift agrees with the chines-wet lift at the critical wetted length, i.e., change 3.6 to 3.05 so that $C_{L_b} = .07$ at $\delta = .0876$. The effect of warp rate on C_{L_b} deserves comment: It has been found that the lift coefficient based on wetted area is slightly greater for the low warp plane than for no warp and much greater for the high warp plane. For a given draft, or keel wetted length, the wetted area of the warped planes is, however, substantially less than for the non-warped hulls. This effect overbalances the higher lift coefficient for the low warp hull and partially balances it for the high warp hull. Eng's analysis[9] for chines-dry planing suggests that C_{L_b} should be somewhat increased by warp for this case but the results exhibited in Fig. 10 do not show this. This may be associated with dependence of wetted area, and especially of the "critical" wetted length, on the warp. For the present report this small discrepancy will not be further investigated. The planing data of Figs. 8 and 9 will be used to represent the influence of the two warp rates and the critical wetted length given by Eq. (48) will be used to evaluate the chines-dry planing performance.

RESULTS AND DISCUSSION

By inspection of the basic differential equations governing the impact, Eq. (3) for smooth water and Eq. (32) for waves, some useful insight into the early stages of the impact can be gleaned. Note that acceleration is proportional to the product of $\dot{y}^2 = (\dot{z}\cos\tau + \dot{s}\sin\tau)^2$ and $d\mu/d\delta$, and that, in the earliest phase of impact, $\dot{z}$ remains relatively uniform. Consequently, since for chines-dry planing C_{L_b}, and therefore $d\mu/d\delta$, is proportional to δ^2, and δ is proportional to time, the acceleration can be expected to rise as the square of the time. The steepness of the rise is of interest and depends on trim (according to Eqs. (22) and (45)) in proportion to $\cos^2\tau(1-\sin\tau)/\sin\tau$, so that higher trim angles tend to reduce the contribution of $d\mu/d\delta$ to the rate of acceleration rise. It also appears to depend on $\cot^2\beta$, thus favoring high deadrise, and inversely on C_{Δ_o}, suggesting the advantage of high beam loading. The influence of trim on acceleration rise is strongly felt in the dependence of $\dot{y}^2$ on $\dot{s}\sin\tau$, and low trims are generally preferable. A slow, flat glide is preferred, in accordance with intuition in this matter. The influence of warp rate cannot be clearly singled out because of the lack of sufficient chines-dry planing data for these hulls, but, tentatively, the chines-wet lessons may be considered; that a little warp reduces the initial rise of acceleration while substantial warp may increase it.

For the impact in waves, a highly significant aspect is the effect of wave motion on the rate of penetration into water. In the initial stages when vertical velocity is essentially constant, the transom draft and, hence, $d\mu/d\delta$, will increase more or less rapidly depending on whether the water surface at the location of contact is rising or falling. For steep waves especially, $\dot{\eta} = -\frac{2\pi A}{\Lambda}(\dot{s} \pm c)\sin 2\pi\left[\frac{s}{\Lambda} + \frac{(\dot{s} \pm c)}{\Lambda}t\right]$ may be of comparable magnitude to the vertical velocity of the craft.

The lessons to be extracted from the initial stages of the impact are, unfortunately, of limited value since the maximum accelerations occur

when the vertical velocity has changed appreciably from its initial value, the virtual mass fraction μ has become significant and the chines may have become immersed. Nonetheless, the steepness of the rise of acceleration may be expected to be related to the peak acceleration, and is of interest in its own right.

Smooth-Water Results

Figure 11 shows a comparison of theory and experiment for the smooth-water impact of the high warp-rate model for a particular set of initial conditions, viz., glide angle, trim, etc. The theoretical calculations have been carried out according to Eqs. (16), (17), and (19), using the planing data (for virtual mass) as shown in Fig. 8. A photograph showing the development of the planing spray, taken near the instant of peak acceleration, is shown along with the oscillographic time history of acceleration and heave. It may be noted that the peak acceleration occurs near the time at which chine wetting occurs. The acceleration time history prediction is about twice the experimentally measured result; a slight time lag of the experiment following the theory is at least partly due to accelerometer response lag. The difference between theory and experiment is felt to be due to inadequate definition of planing lift data, especially for the vital chines-wet condition. The observed discrepancy between theoretical and experimental heave motion is in line with the differences in acceleration.

Comparisons of theory and experiment for the low warp rate plane are shown in Figs. 12 and 13 for two sets of initial conditions. The planing data of Fig. 9 was used for the calculations and, again, the peak accelerations occur near the time at which chine wetting occurs. This coincidence is not expected to be valid for all impacts inspite of its arising for the three cases of Figs. 11, 12 and 13. For the low warp rate hulls, the theory predicts peak impact accelerations about 30 percent higher than are experienced, with the experiments again showing a slight time lag. The calculated heave motion is less than the measured for these cases also. The case of Fig. 12, with higher trim than the case of Fig. 13, has a somewhat steeper glide path, and the impact loading is also somewhat higher.

Wave Tests

Landings were made in regular waves of two different periods, or lengths, 1.00 sec (Λ=61.5 in) and 1.40 sec (Λ=120.5 in). The wave steepness, or maximum slope, was approximately the same for all tests, varying over the range from 5.5 deg to 6.6 deg. The landing direction was always towards the oncoming waves.

For a given trim angle and glide path the presence of waves generally produces a decidedly unfavorable increase in the impact loadings, especially for landings against an oncoming wave front. For landings on the receding side of the wave, where the water elevation is falling, it is possible to obtain less than smooth-water impacts, but to achieve this type of landing is not easy since for any glide path the "window for landing on the rising wave face is much wider than the "window" for landing on the falling-away face (see sketch).

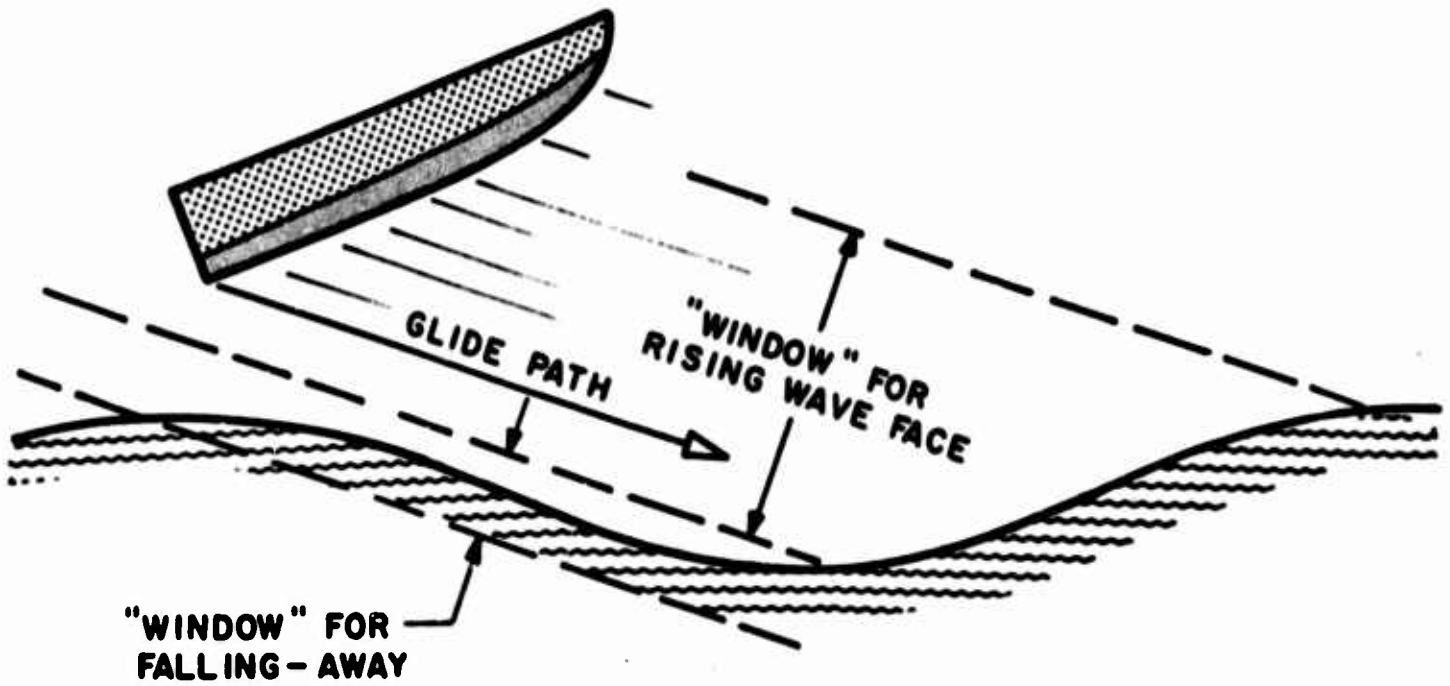

A sequence of landings at different positions on the oncoming wave front is illustrated in Fig. 14. Here the oscillograms of acceleration are shown for several landings in waves of length Λ = 120.5 inches of the low-warp plane, at 4 deg trim and with glide angle (arctan $\dot{z}/\dot{s}$) between 10.6 and 12.7 deg. Also shown are photographs of the spray pattern obtained during some of these impacts. The variation of the peak acceleration with the location of initial contact with the wave is very great

indeed, emphasizing the importance of carefully considering the influence of waves on landing. For the tests shown, the trim angle is less than the maximum wave slope; consequently, the implicit assumption that the transom point contacts the water first may be violated. (Alternately, the effective trim angle $\gamma = \tau - d\eta/d\xi$ may be negative, a case for which planing data and therefore added mass information cannot be obtained by the present techniques.) For some impacts, through the 'window' for falling-away wave face for instance, the theory should still describe the initial stages of impact, until the advance of wave and hull results in the forward part of the plane being buried in the oncoming wave ($\gamma \leq 0$).

Figure 15 shows peak acceleration values for several other sets of impacts, including the high warp plane in waves of length $\Lambda = 120.5$ in. and 61.5 in. and the low warp plane in waves with $\Lambda = 61.5$ in. The trim angle τ of 4 deg in all cases is again less than the maximum wave slope. It is also apparent for these cases that the effect of the wave is great. It appears to be of greater significance for the low warp plane than for the high warp plane: From Figs. 14 and 15, it can be seen that the ratio of the greatest peak acceleration for landing in waves to the peak acceleration for landing in smooth water is about 10.5/3.1 = 3.4 for the low warp plane and only 5.5/2.2 = 2.5 for the high warp plane. These results depend, of course, on model displacement, glide path, trim angle, and wave length and steepness, so that a generally applicable rule cannot be given on the basis of the experimental results alone.

The calculation of impact in waves according to the theory (of Eqs. (17) and (38)-(44)) has not been accomplished at the present time. Some evaluations of the very early stages of the impact, using the basic differential Eq. (32) derived taking account of wave kinematics, have been carried out for cases where $\tau - d\eta/d\xi > 0$. Results are shown for cases of both high and low warp planes in Fig. 16, along with experimentally-recorded oscillograms. The agreement between theory and experiment indicates the probable validity of the derived differential Eq. (32).

Further analysis and numerical evaluation of the solution for the complete time history should be carried out. The analysis, in fact, should be extended to permit assessment of certain other influences, the most

significant of which are the effect of partial wing support of the aircraft and the possibility of rotational (pitching) motion of the craft occurring during, but not necessarily due to, the impact.

CONCLUSIONS AND RECOMMENDATIONS

Study of water impact of planing surfaces has been carried out along the lines of Brown's[1] analysis procedure. The analysis has been extended to the case of landing in waves by taking account of the wave kinematics in the development of the differential equation of motion. Experiments have been conducted with two models having different amounts of warp or longitudinal variation of deadrise. Planing data are used to derive virtual mass information which is needed in the evaluation of the theory.

For smooth water impacts the analysis, together with the planing data for added mass, suggests that increased warp rate tends to increase the rate-of-acceleration rise and, probably, the peak acceleration, for craft of equal displacement. Comparison of impact tests with analytical results for smooth water indicate that the planing data for the high warp rate model give added mass values which are too high for the chines-dry case. Since this information was obtained by extrapolation from chines-wet planing data, it is uncertain anyway and ought to be obtained by special chines-dry planing tests with variable deadrise surfaces. Comparison of theory and experiment for impact tests of the low warp rate model are in better agreement, but suggest that the chines-dry added mass is somewhat overestimated by the extrapolated planing data for this surface too.

Experimental results reveal the great importance of the waves on the peak impact accelerations and their time histories. The position on the wave at which the craft contacts the water is crucially important and while landing against a rising wave face increases the peak acceleration drastically, the accelerations experienced in landing on the falling-away wave face can be less than those for landing in smooth water. It is intuitively clear that landing against a rising wave face is more likely to occur than landing on a falling-away wave face, however.

Complete calculations for impact in waves have not yet been carried out. Some evaluations of the early stages of the impact, before the vertical velocity begins to change significantly, indicate reasonable

correlation with the experimental oscillograms, suggesting that the differential equation derived taking account of wave kinematics may be appropriate. The trim angle of the craft relative to the horizontal ought to be greater than the maximum wave slope in order to avoid "flat-bottom" slamming onto an oncoming wave front and attendant high impact accelerations.

It is recommended that calculations according to the derived theory be carried out for the complete time history of landings in waves. The analysis ought to be extended to include only partial wing lift and the occurrence of pitching motion of the craft during, but not necessarily due to, the impact.

REFERENCES

1. Brown, P.W., "Seaplane Impact Theory." Short Brothers and Harland Limited, Hydrodynamics Note No. 46, August 1954.

2. Smiley, R.F., "The Application of Planing Characteristics to the Calculation of the Water-Landing Loads and Motions of Seaplanes of Arbitrary Constant Cross Section." NACA TN 2814, November 1952.

3. Monaghan, R.J. and Crewe, P.R., "Formulae for Estimating the Forces in Seaplane-Water Impacts Without Rotation or Chine Immersion." ARC R&M 2804, London, 1955.

4. Brown, P.W., "An Empirical Analysis of the Planing Characteristics of Rectangular Flat Plates and Wedges." Short Brothers and Harland Limited, Hydrodynamics Note No. 47, September 1954.

5. Milne-Thomson, L.M., Theoretical Aerodynamics, 3rd Ed., MacMillan & Company, Ltd., New York, 1958, p.224.

6. Brown, P.W., "Characteristics of Planing Surfaces Fitted With Transom Flaps." Stevens Institute of Technology, Davidson Laboratory, Report 1522 [to be published].

7. Shuford, C.L., Jr., "A Theoretical and Experimental Study of Planing Surfaces Including the Effect of Cross Section and Plan Form." NACA TN 3939, November 1956.

8. Eng, K., "A Preliminary Study of Smooth-Water Impact Theory for Chines-Dry Warped Surfaces." Stevens Institute of Technology, Davidson Laboratory, Report 1374, February 1969.

TABLE I

$$\varphi = me^{1/m}$$

m	0	1	2	3	4	5	6	7	8	9
0	∞									
0.10	2202.7									
0.20	29.683									
0.30	8.4096									
0.40	4.8730	4.6993	4.5424	4.4000	4.2706	4.1525	4.0446	3.9457	3.8550	3.7715
0.50	3.6945	3.6235	3.5578	3.4970	3.4407	3.3884	3.3397	3.2946	3.2525	3.2133
0.60	3.1767	3.1426	3.1108	3.0807	3.0533	3.0173	3.0031	2.9804	2.9592	2.9394
0.70	2.9209	2.9036	2.8875	2.8724	2.8584	2.8452	2.8330	2.8217	2.8111	2.8013
0.80	2.7923	2.7839	2.7761	2.7690	2.7625	2.7565	2.7510	2.7461	2.7416	2.7376
0.90	2.7340	2.7308	2.7280	2.7256	2.7236	2.7219	2.7206	2.7196	2.7188	2.7184
1.00	2.1783	2.7184	2.7188	2.7195	2.7203	2.7215	2.7228	2.7244	2.7261	2.7281
1.10	2.7303	2.7326	2.7351	2.7379	2.7407	2.7438	2.7469	2.7503	2.7538	2.7574
1.20	2.7612	2.7651	2.7691	2.7733	2.7775	2.7819	2.7864	2.7911	2.7958	2.8006
1.30	2.8055	2.8106	2.8157	2.8209	2.8262	2.8316	2.8371	2.8427	2.8483	2.8540
1.40	2.8598	2.8657	2.8716	2.8777	2.8837	2.8899	2.8961	2.9024	2.9087	2.9151
1.50	2.9216	2.9281	2.9347	2.9413	2.9480	2.9548	2.9615	2.9684	2.9753	2.9822
1.60	2.9892	2.9962	3.0033	3.0104	3.0176	3.0248	3.0320	3.0393	3.0466	3.0540
1.70	3.0641	3.0691	3.0763	3.0638	3.0913	3.0989	3.1065	3.1141	3.1218	3.1295
1.80	3.1372	3.1450	3.1528	3.1606	3.1684	3.1763	3.1842	3.1922	3.2001	3.2091
1.90	3.2161	3.2241	3.2322	3.2403	3.2484	3.2565	3.2646	3.2728	3.2810	3.2892
2.00	3.2974	3.3057	3.3140	3.3223	3.3306	3.3389	3.3473	3.3556	3.3640	3.3724
2.10	3.3809	3.3893	3.3978	3.4062	3.4147	3.4232	3.4318	3.4403	3.4489	3.4574
2.20	3.4660	3.4736	3.4832	3.4919	3.5005	3.5092	3.5178	3.5265	3.5352	3.5439
2.40	3.6406	3.6494	3.6583	3.6671	3.6760	3.6849	3.6938	3.7028	3.7117	3.7026
2.50	3.7296	3.7385	3.7475	3.7565	3.7654	3.7744	3.7834	3.7924	3.8015	3.8105
2.60	3.8195	3.8286	3.8376	3.8467	3.8558	3.8648	3.8739	3.8830	3.8921	3.9012
2.70	3.9103	3.9195	3.9286	3.9377	3.9469	3.9560	3.9652	3.9743	3.9835	3.9927
2.80	4.0019	4.0111	4.0203	4.0295	4.0387	4.0479	4.0571	4.0663	4.0756	4.0848
2.90	4.0941	4.1033	4.1126	4.1218	4.1311	4.1404	4.1497	4.1589	4.1682	4.1775
3.00	4.1868	4.1961	4.2055	4.2148	4.2241	4.2334	4.2428	4.2521	4.2614	4.2708
3.10	4.2801	4.2895	4.2988	4.3082	4.3176	4.3269	4.3363	4.3457	4.3551	4.3645
3.20	4.3739	4.3833	4.3927	4.4021	4.4115	4.4209	4.4303	4.4398	4.4492	4.4586
3.30	4.4681	4.4775	4.4869	4.4964	4.5058	4.5153	4.5247	4.5342	4.5437	4.5531
3.40	4.5626	4.5721	4.5816	4.5910	4.6005	4.6100	4.6195	4.6290	4.6385	4.6480
3.50	4.6575	4.6670	4.6765	4.6860	4.6955	4.7051	4.7146	4.7241	4.7336	4.7432
3.60	4.7527	4.7622	4.7718	4.7813	4.7909	4.8004	4.8100	4.8195	4.8291	4.8386
3.70	4.8482	4.8577	4.8673	4.8769	4.8864	4.8960	4.9056	4.9152	4.9248	4.9343
3.80	4.9439	4.9535	4.9631	4.9727	4.9823	4.9919	5.0015	5.0111	5.0207	5.0303
3.90	5.0399	5.0495	5.0591	5.0687	5.0784	5.0880	5.0976	5.1072	5.1168	5.1265
4.0	5.1361									
5.0	6.1070									
6.0	7.0882									
7.0	8.0750									
8.0	9.0652									
9.0	10.058									
10.0	11.052									

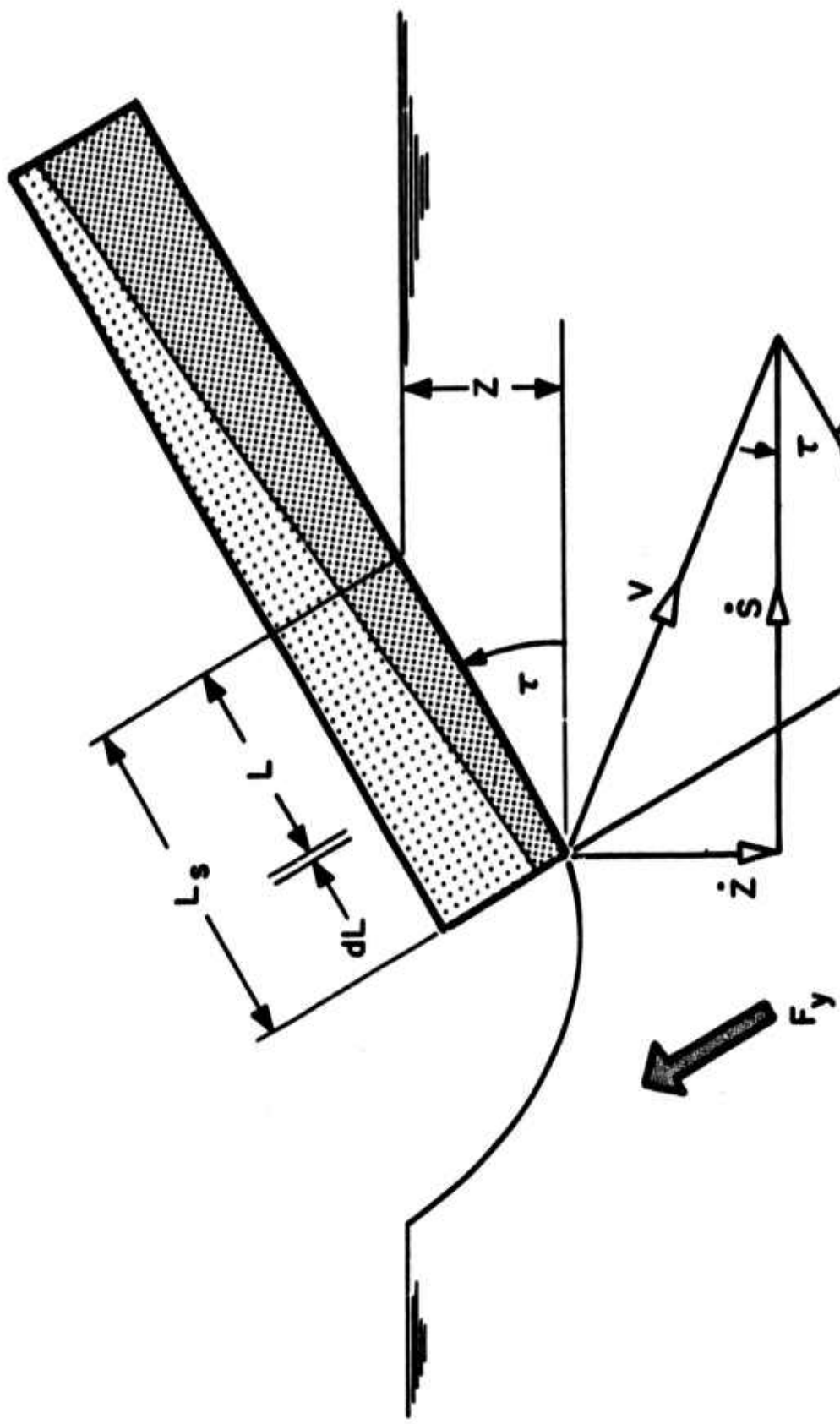

FIG. I. OBLIQUE STEP IMPACT

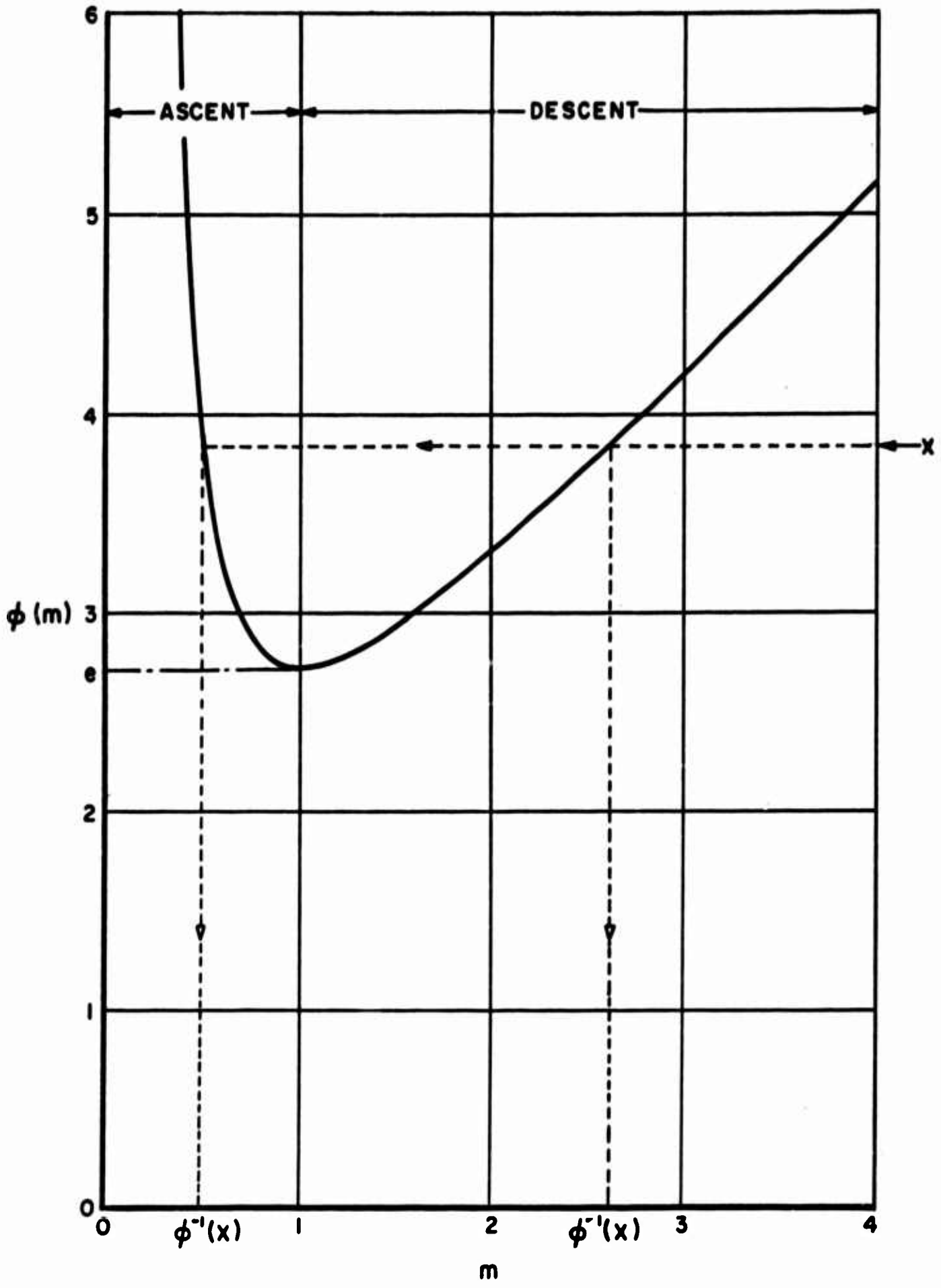

FIG. 2. ϕ – FUNCTION, $\phi(m) = m e^{1/m}$

$$\eta = A \cos 2\pi \left[\frac{\xi}{\lambda} + \frac{(\dot{s} \pm c)}{\lambda} t \right]$$

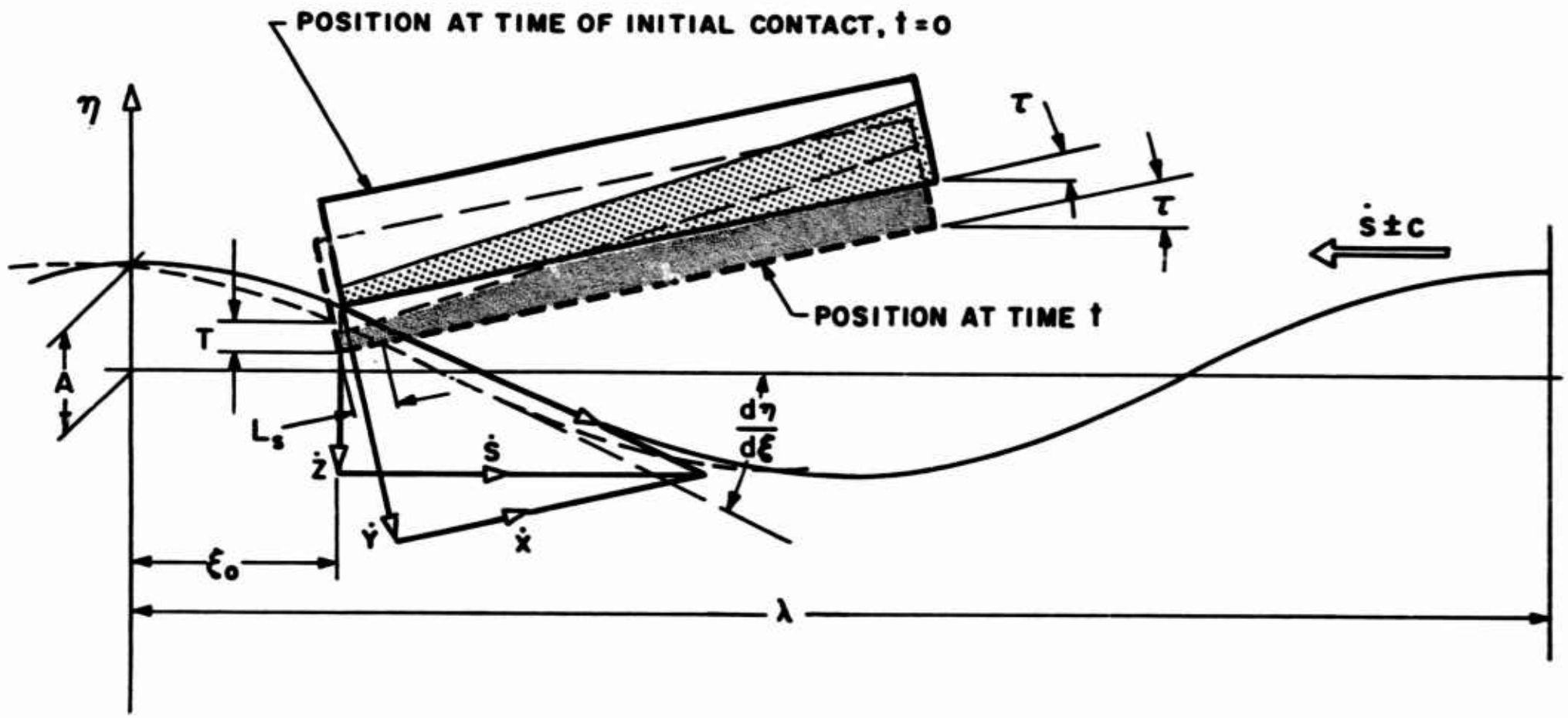

R-1514

FIG. 3. KINEMATICS FOR IMPACT IN WAVES

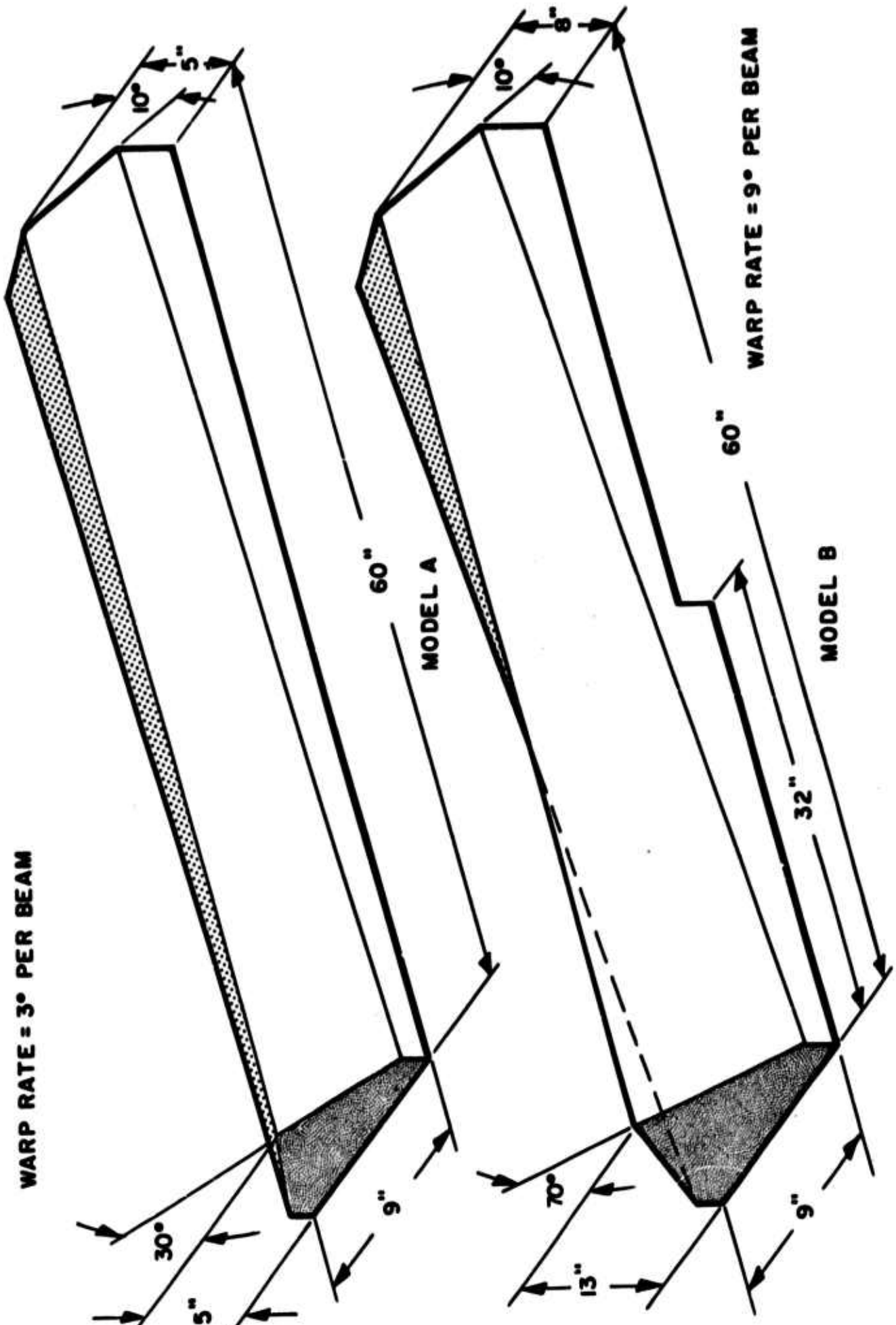

FIG. 4. WARPED SURFACE PLANING HULLS USED IN EXPERIMENT

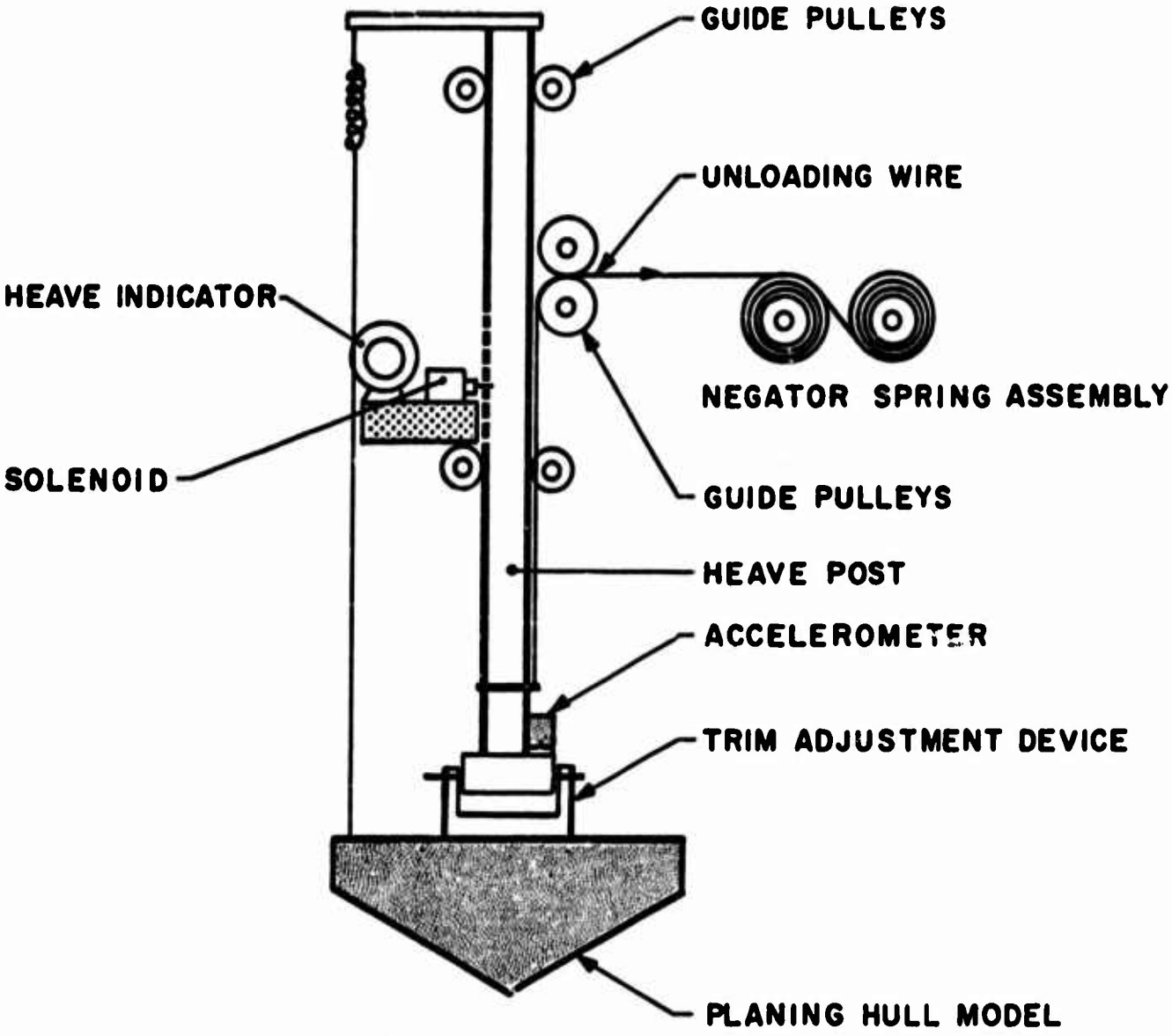

FIG. 5. SCHEMATIC OF IMPACT APPARATUS

IMPACT APPARATUS

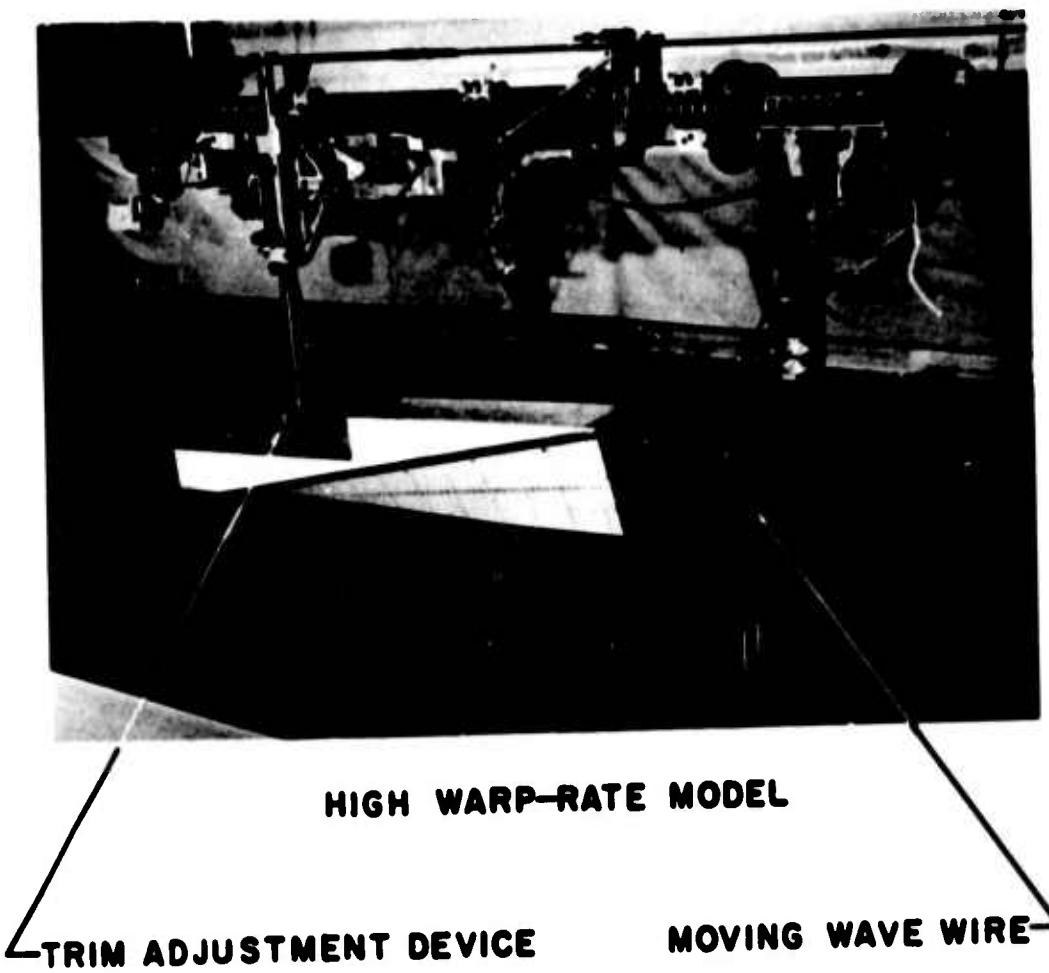

FIG. 6. PHOTO OF APPARATUS AND TEST SET-UP

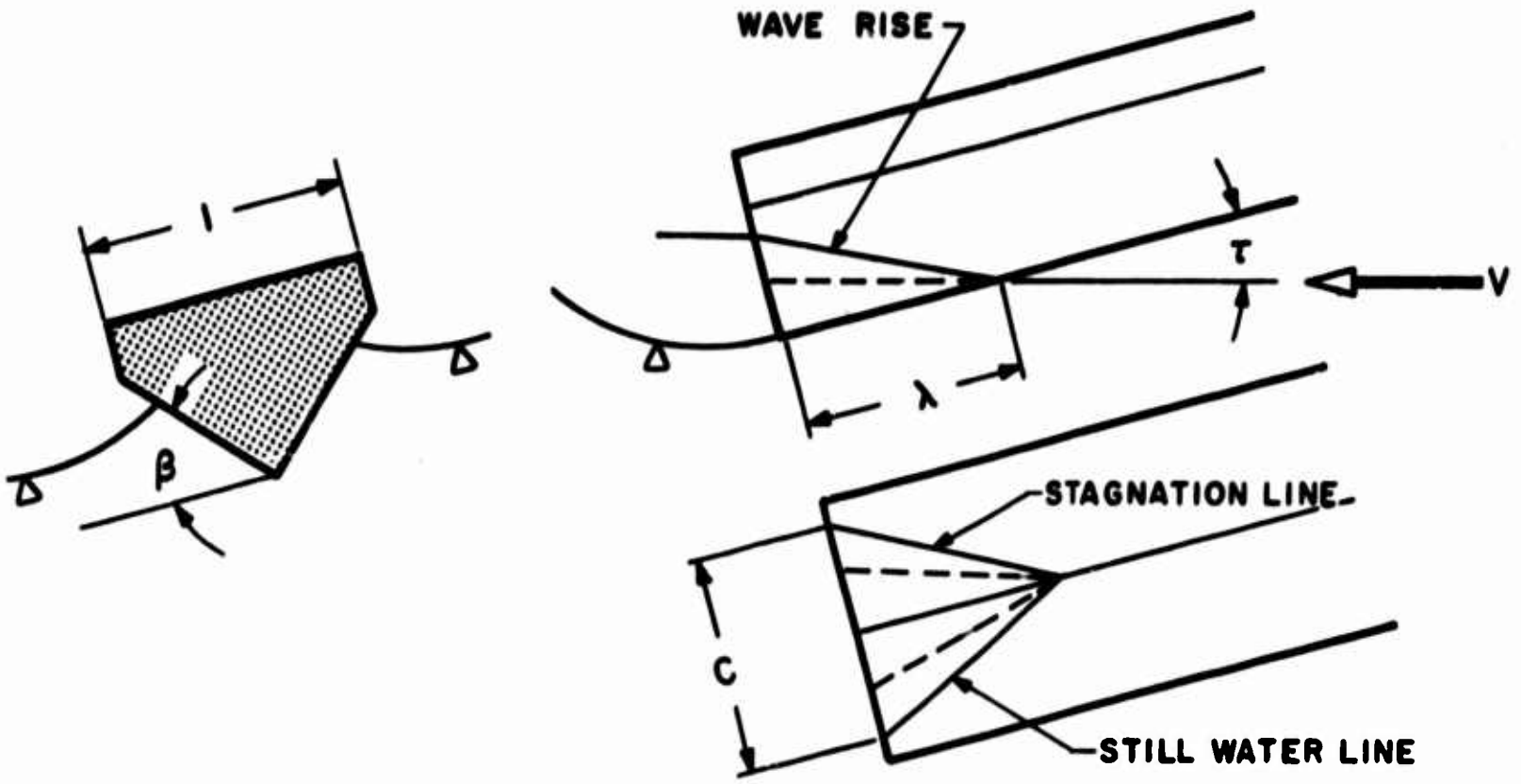

(A) CHINES-DRY PLANING

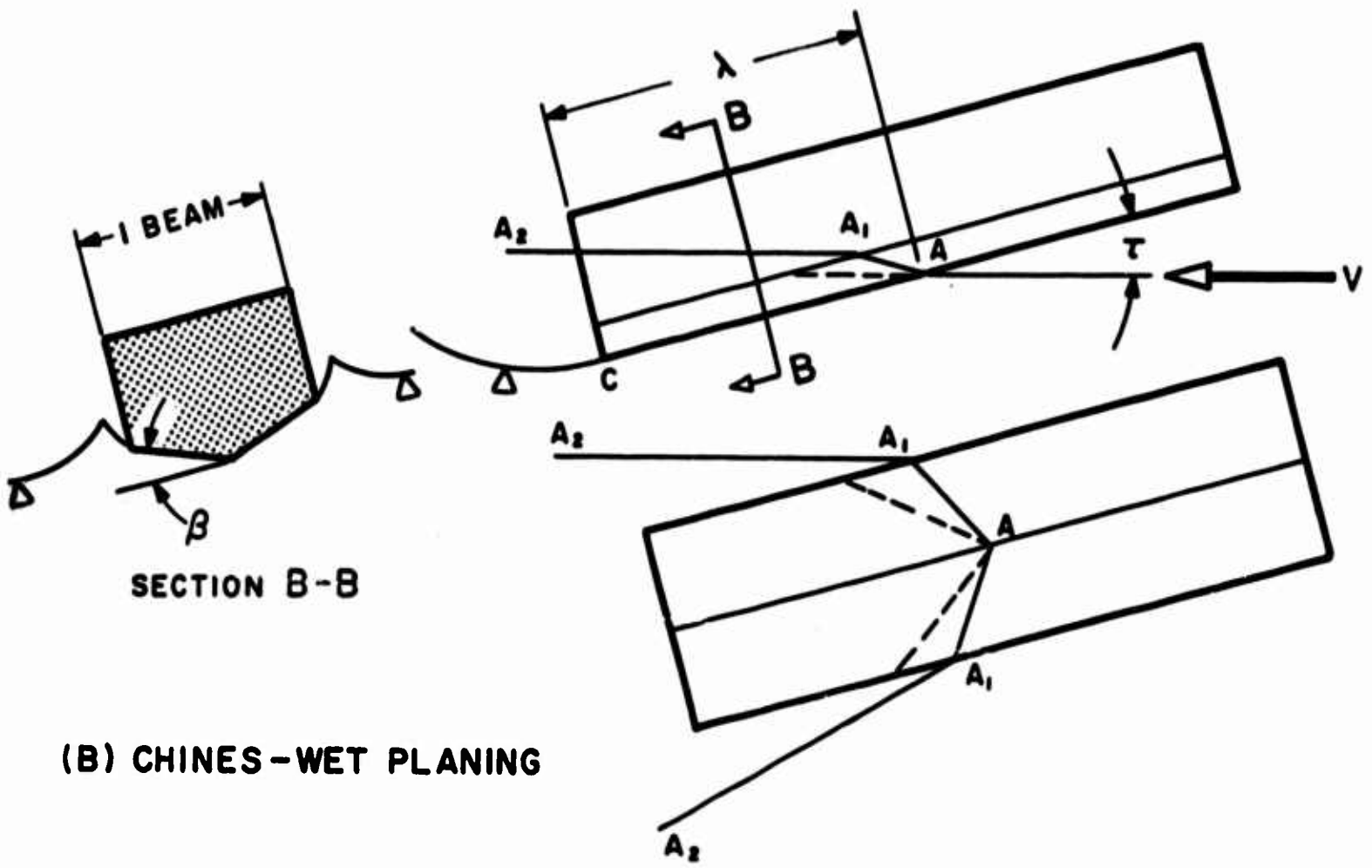

(B) CHINES-WET PLANING

FIG. 7. GEOMETRIES OF PLANING CONDITIONS

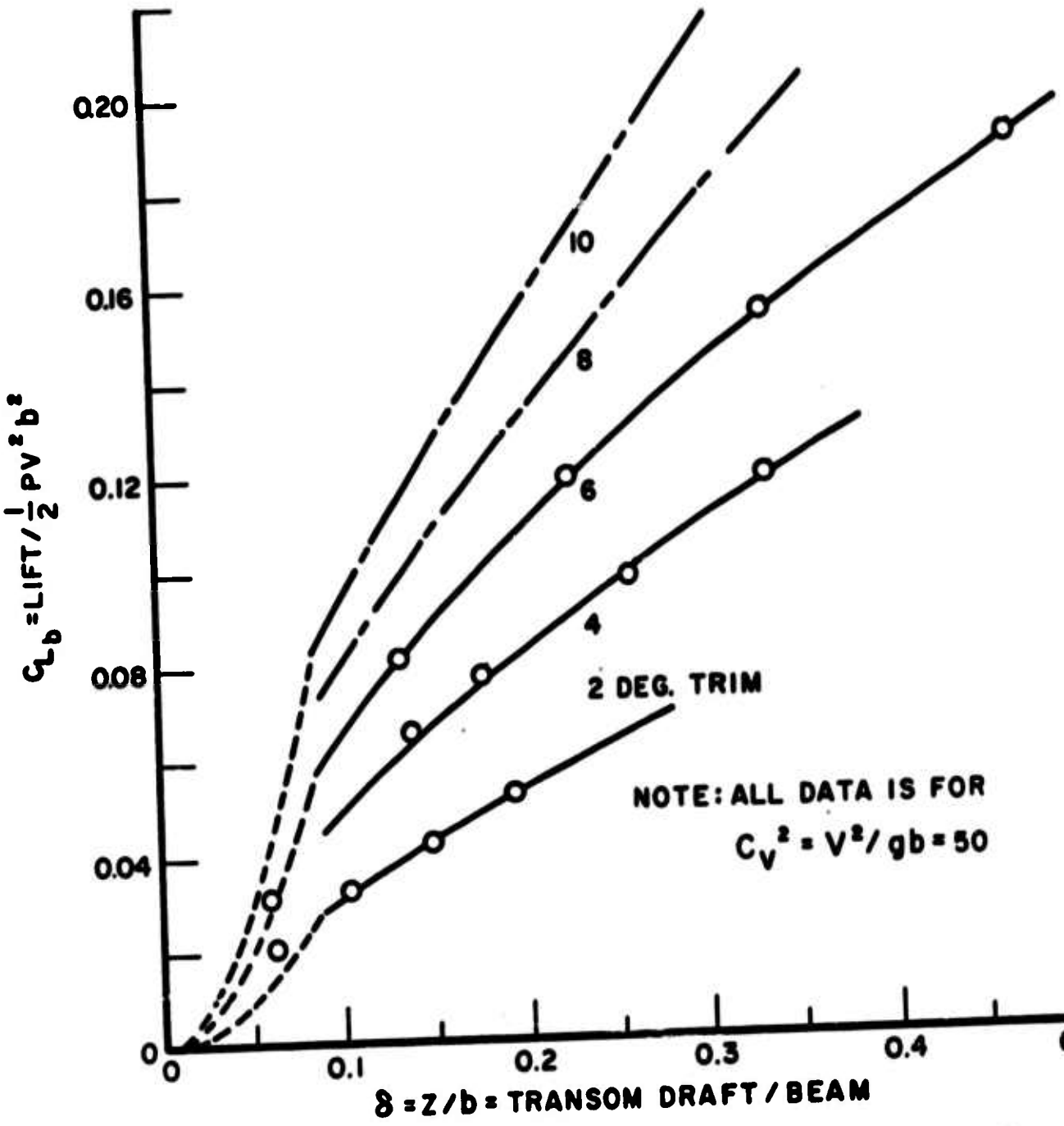

FIG. 8. PLANING LIFT DATA FOR LOW WARP RATE HULL (3 DEG. / BEAM)

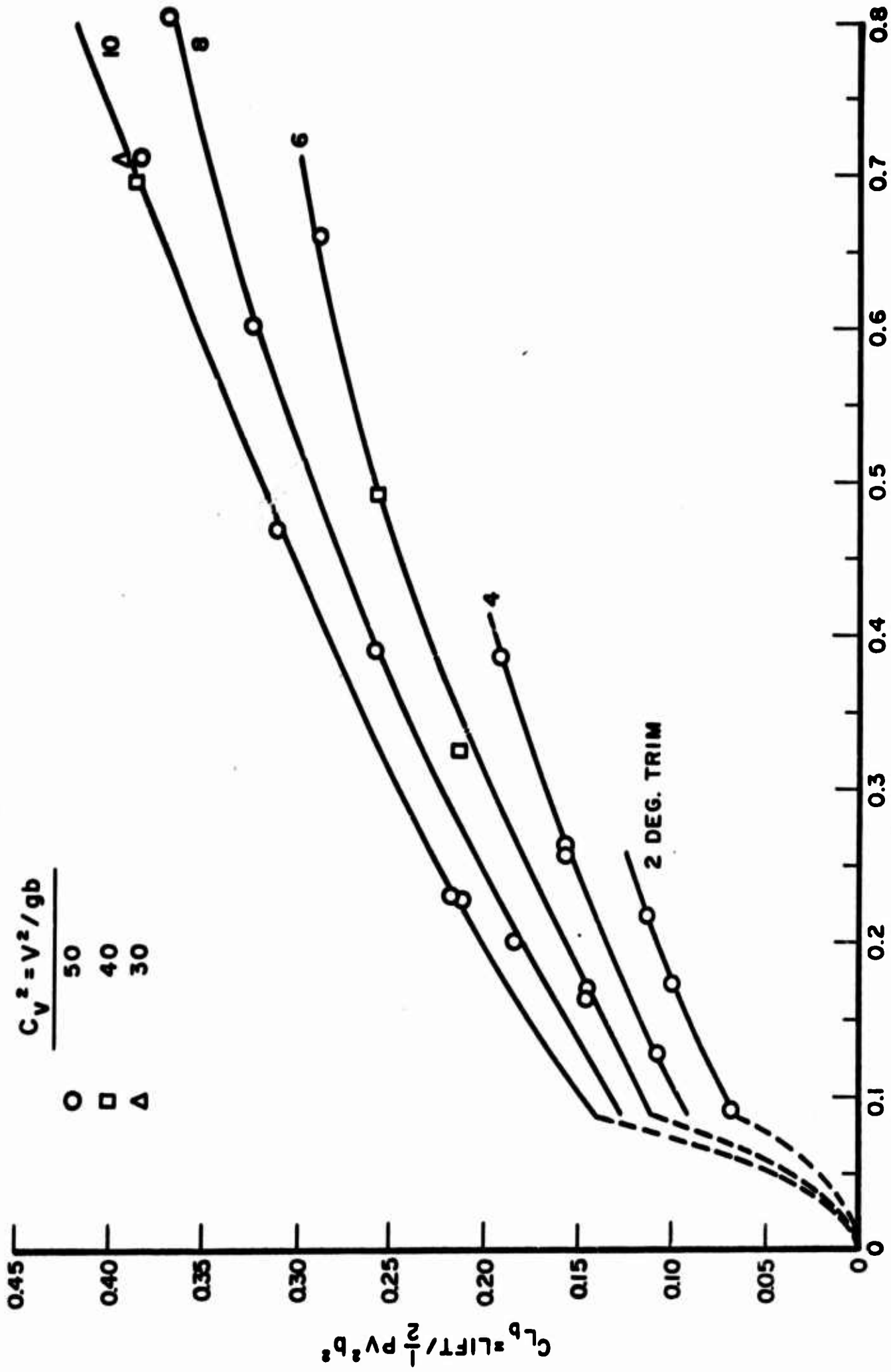

FIG. 9. PLANING LIFT DATA FOR HIGH WARP RATE HULL (9 DEG/BEAM).

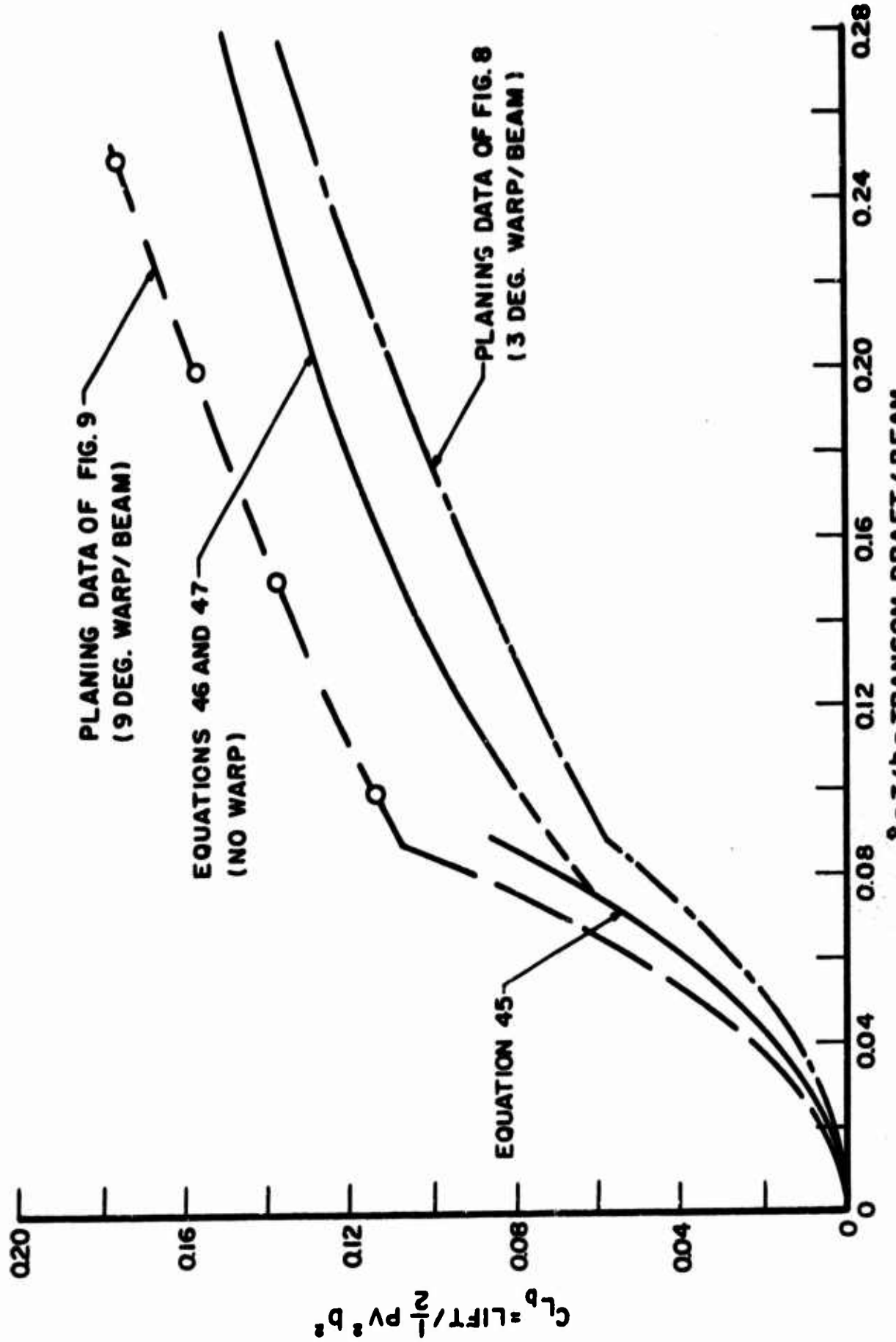

FIG. 10. INFLUENCE OF HULL WARP ON PLANING LIFT.

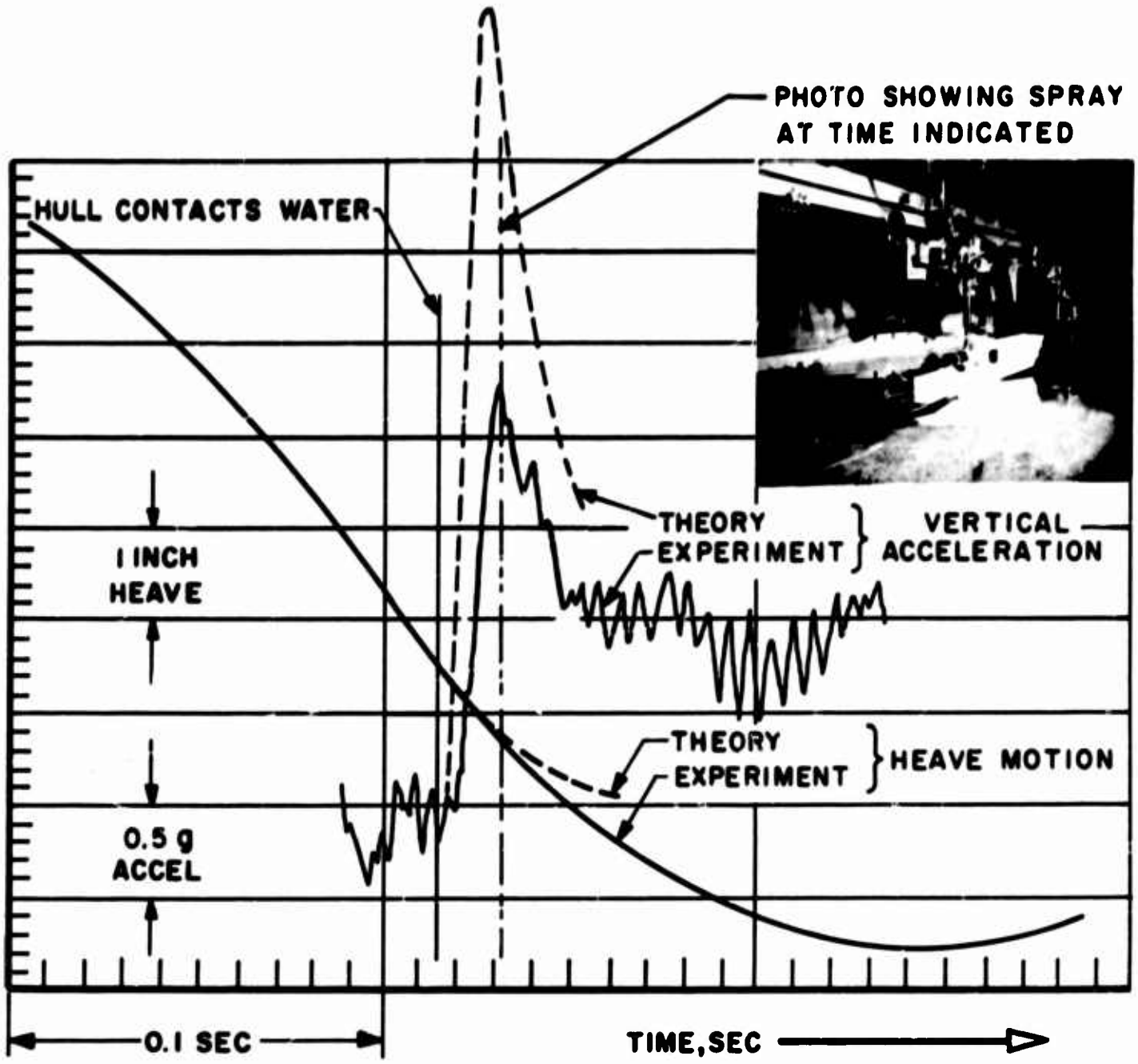

HIGH WARP PLANE (TEST RUN 30)
TRIM = 5 DEGREES
HORIZONTAL VELOCITY, $\dot{S}$ = 20.40 FT/SEC
INITIAL VERTICAL VELOCITY, $\dot{Z}_0$ = 4.33 FT/SEC
Δ_0 = 34.2 LBS

FIG. 11. COMPARISON OF THEORY AND EXPERIMENT FOR SMOOTH-WATER IMPACT OF PLANING SURFACE.

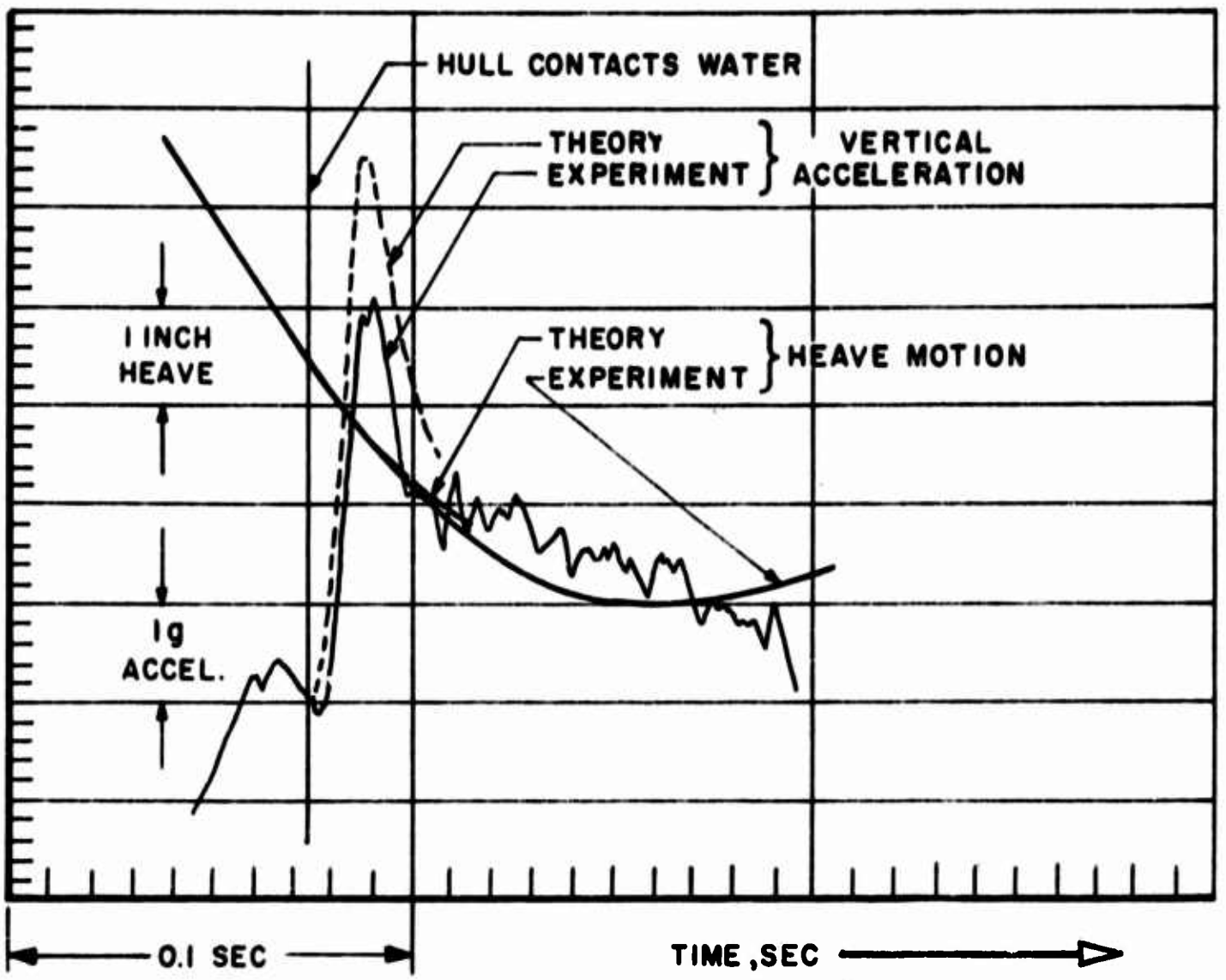

LOW WARP PLANE (TEST RUN 8)
TRIM = 5 DEGREES
HORIZONTAL VELOCITY, $\dot{S}$ = 20.20 FT/SEC
INITIAL VERTICAL VELOCITY, $\dot{Z}_0$ = 5.17 FT/SEC
Δ_0 = 19.6 LBS

FIG. 12. COMPARISON OF THEORY AND EXPERIMENT FOR SMOOTH-WATER IMPACT OF PLANING SURFACE.

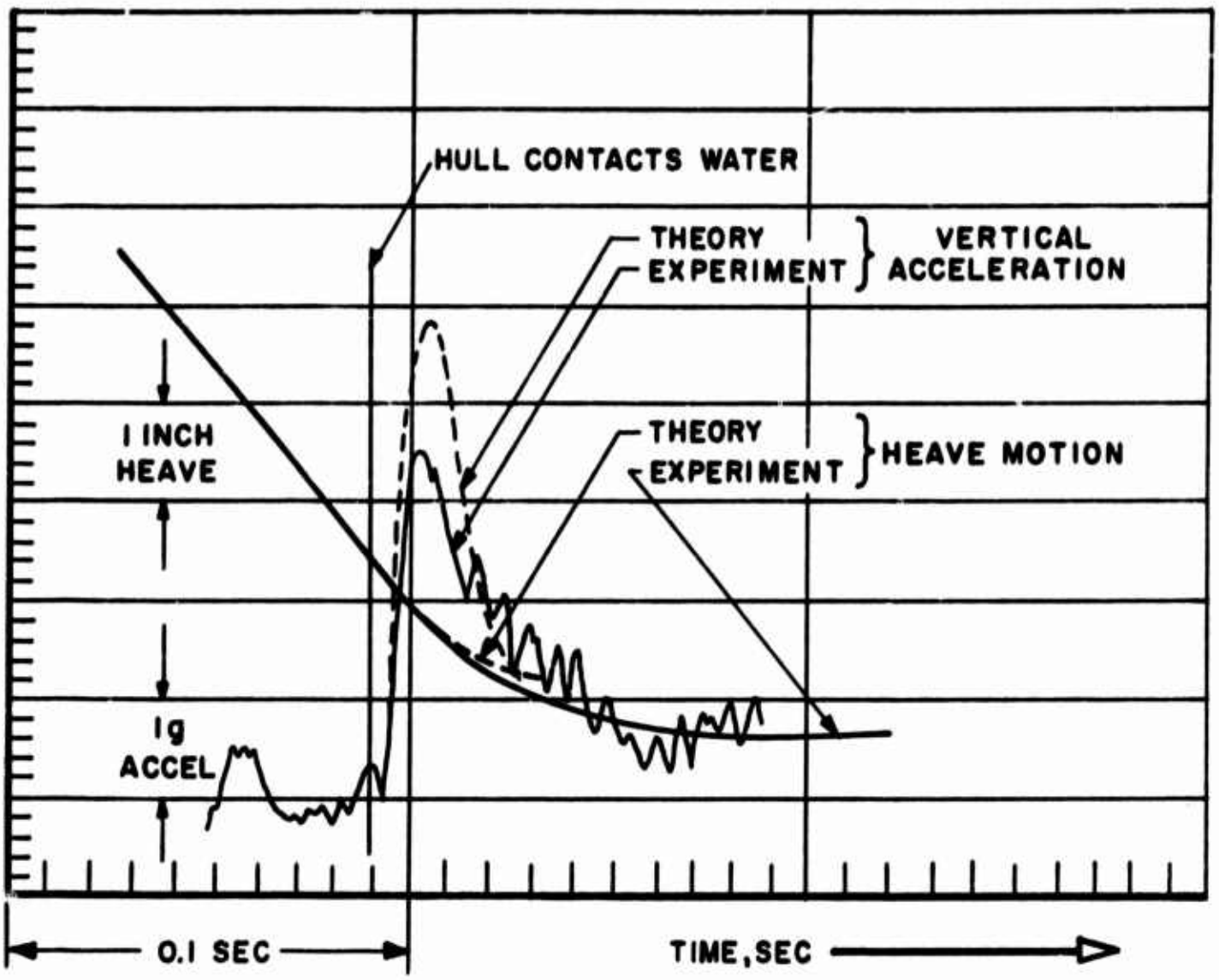

LOW WARP PLANE (TEST RUN 9)
TRIM≈2 DEGREES
HORIZONTAL VELOCITY, $\dot{S}$ = 20.20 FT/SEC
INITIAL VERTICAL VELOCITY, $\dot{Z}_0$ = 4.20 FT/SEC
Δ_0 = 19.6 LBS

FIG. 13. COMPARISON OF THEORY AND EXPERIMENT FOR SMOOTH-WATER IMPACT OF PLANING SURFACE.

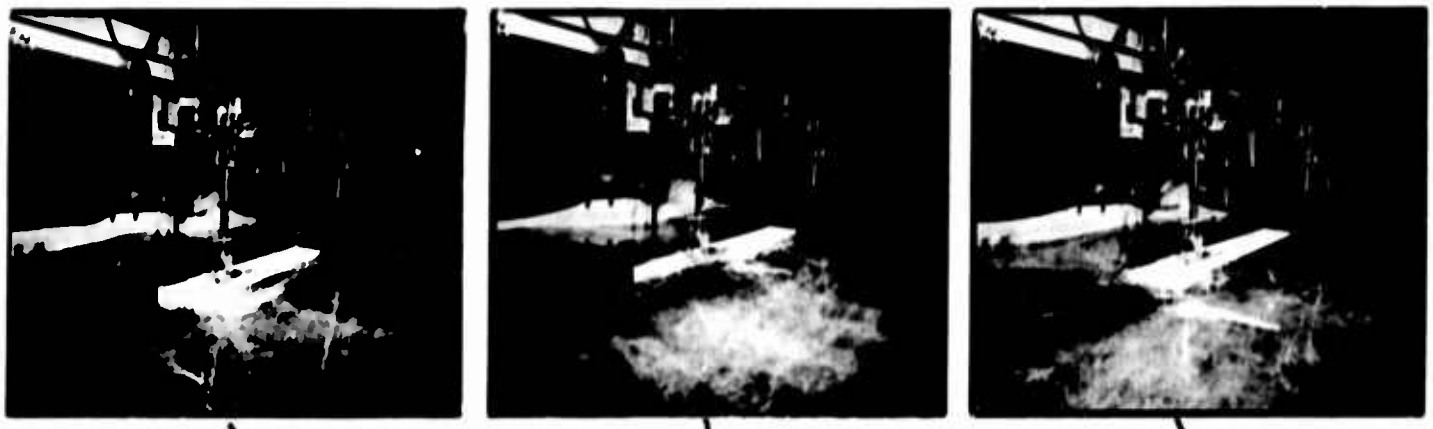

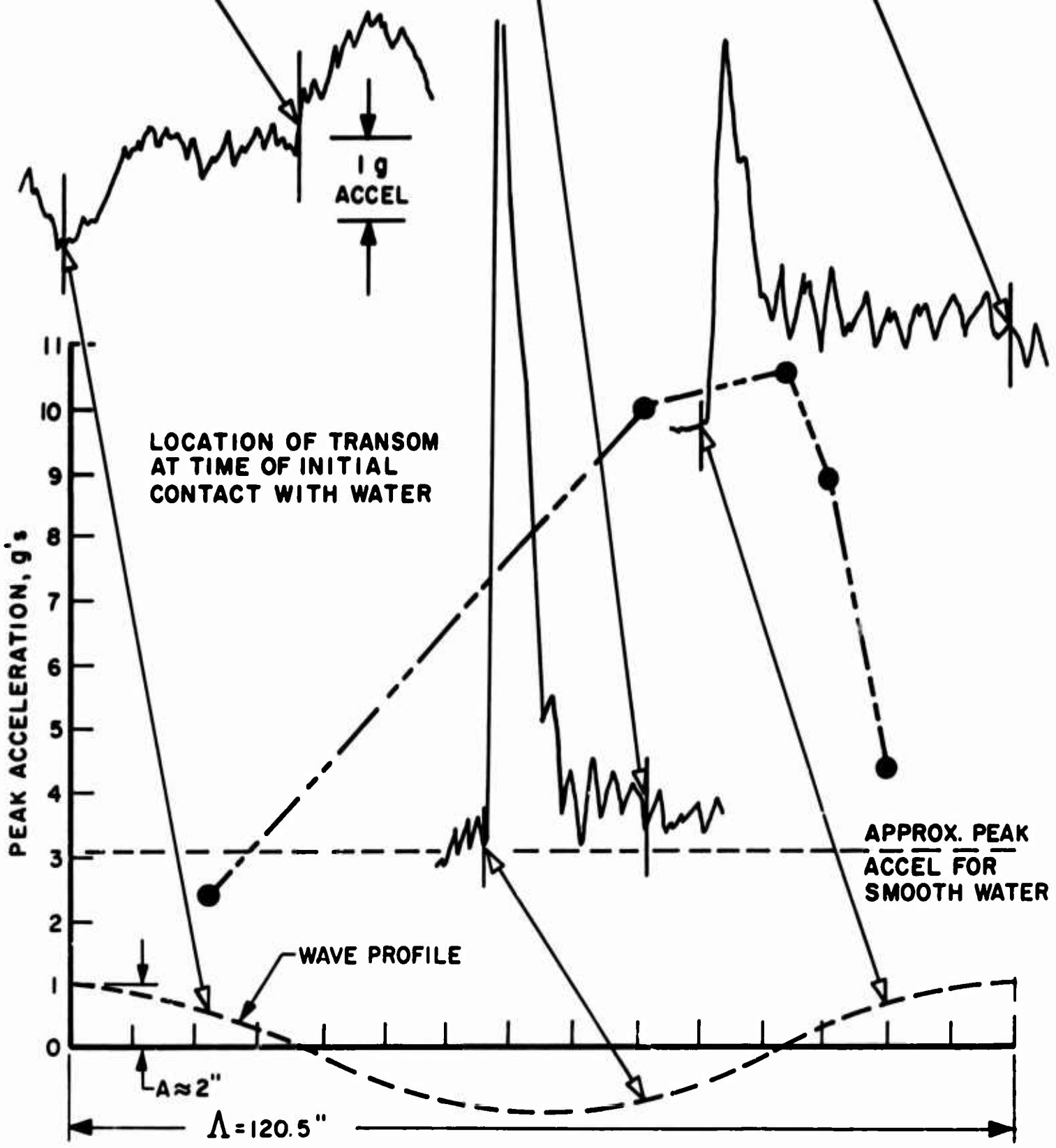

FIG. 14. LANDING IMPACTS IN WAVES
TRIM = 4 DEG, GLIDE ANGLE = 10.6 TO 12.7 DEG

	MODEL	Λ	GLIDE ANGLE	TRIM	Δ_o	$\dot{S}_o$
○	HIGH WARP	120.5 IN.	11.2-13.1 DEG.	4 DEG.	34.2 LB.	20.2 FT/SEC
□	HIGH WARP	61.5 IN.	11.5-12.2 DEG.	4 DEG.	34.2 LB.	20.4 FT/SEC
△	LOW WARP	61.5 IN.	10.9-11.5 DEG.	4 DEG.	19.6 LB.	20.4 FT/SEC

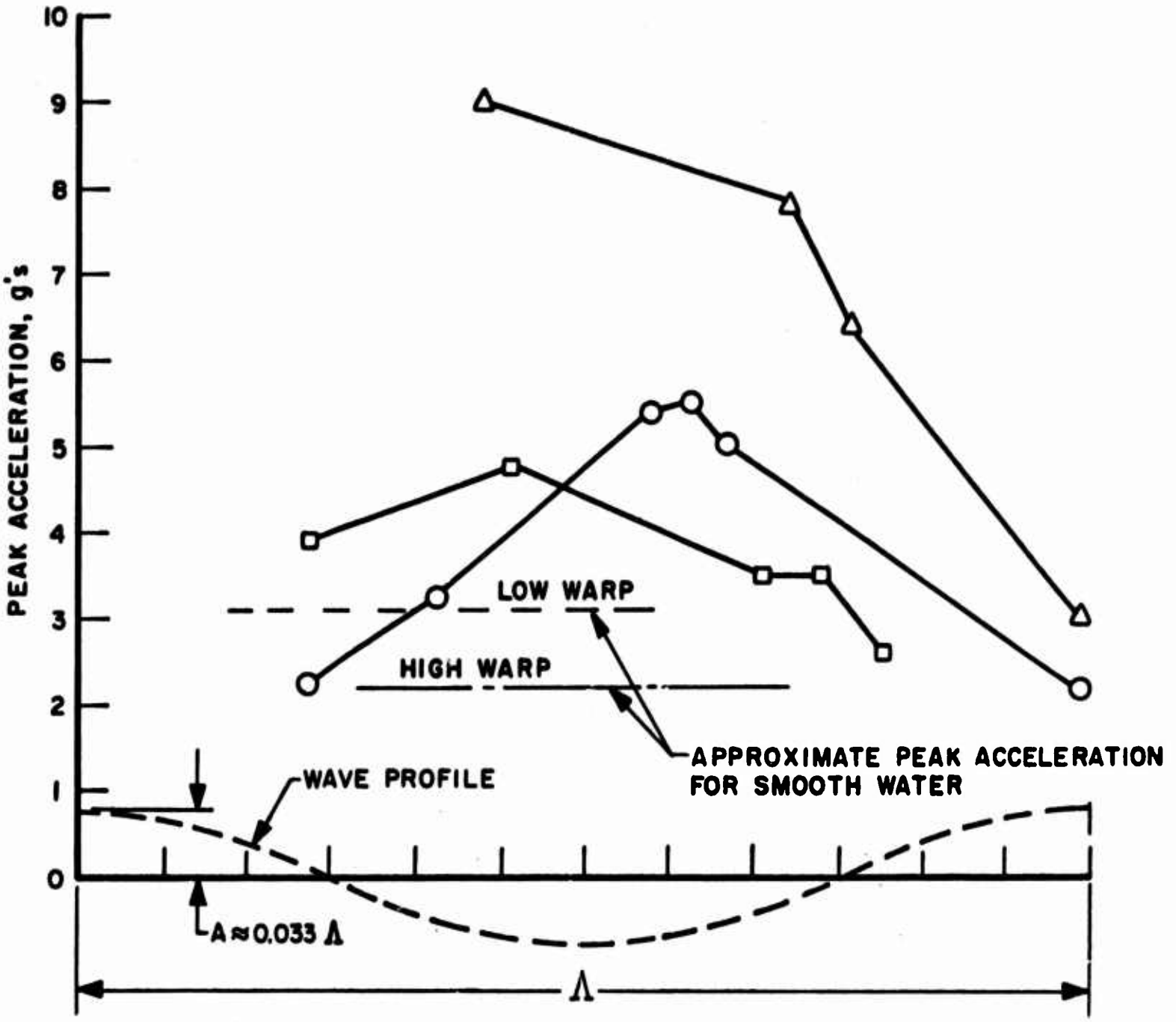

FIG. 15. LANDING IMPACTS IN WAVES

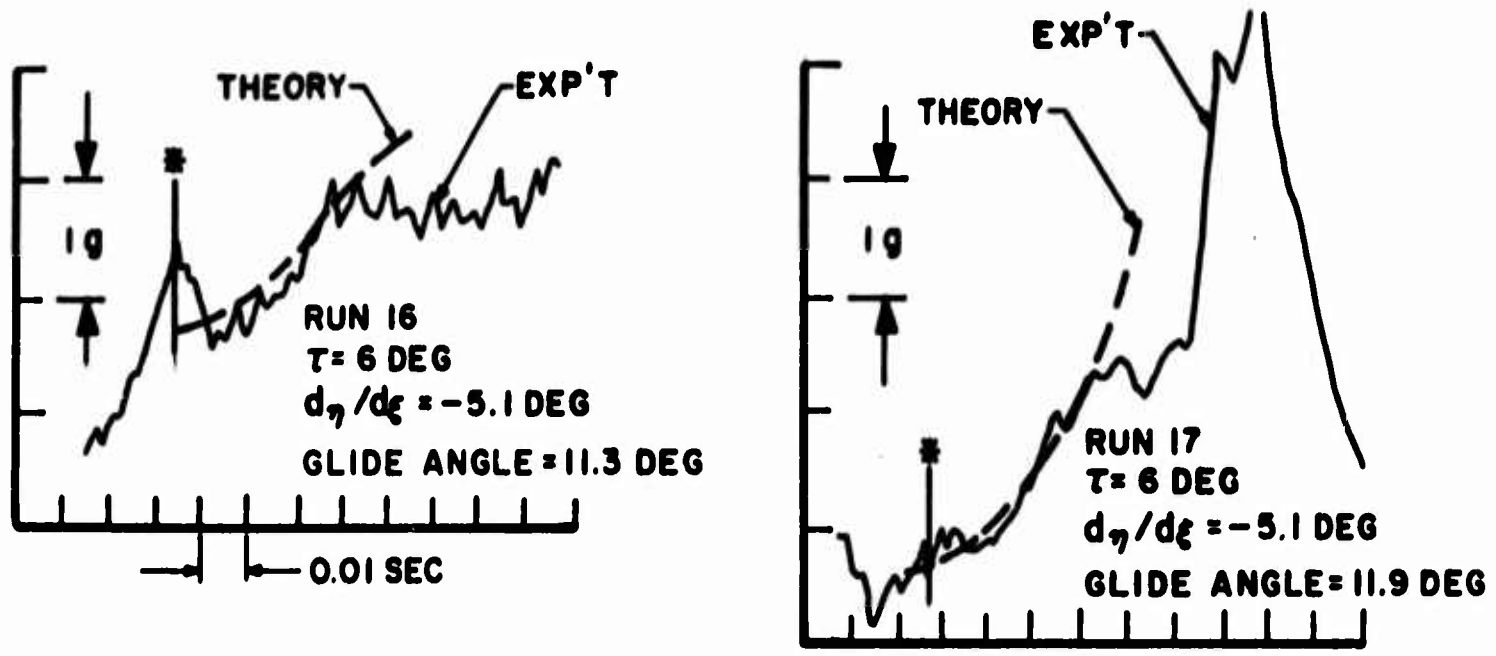

LOW WARP MODEL

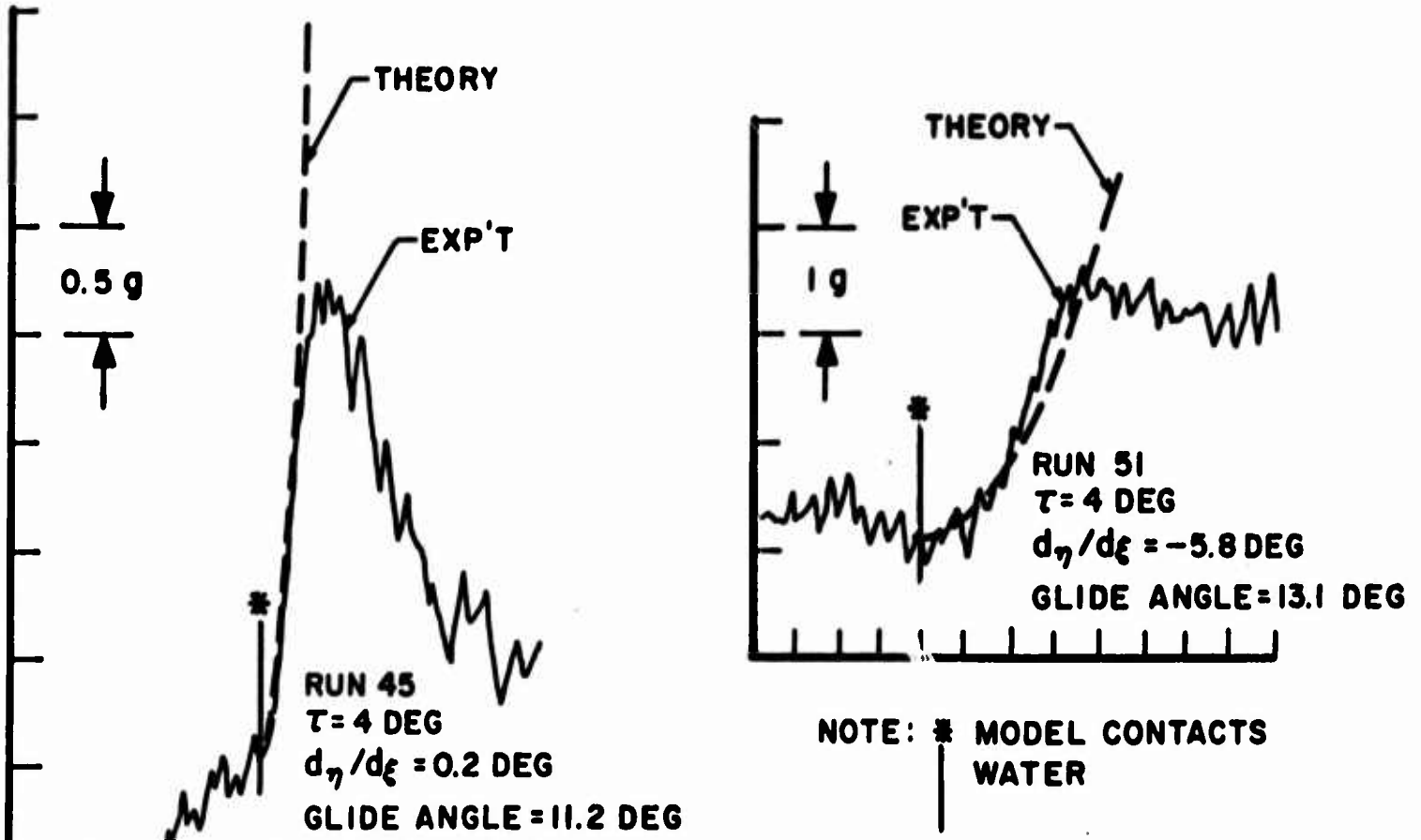

HIGH WARP MODEL

FIG. 16. TIME HISTORIES OF LANDING IMPACTS IN WAVES. COMPARISON WITH THEORY FOR INITIAL STAGES OF LANDING (EQ. 32 WITH y = CONST.) $\dot{s}$ = 20.4 FT/SEC Λ = 120.5 IN. FOR ALL.